

DIGITAL ACCESS TO SCHOLARSHIP AT HARVARD
DASH.HARVARD.EDU

HARVARD LIBRARY


The cold-induced lipokine 12,13-diHOME promotes fatty acid transport into brown adipose tissue

Citation

Lynes, Matthew D, Luiz O Leiria, Morten Lundh, Alexander Bartelt, Farnaz Shamsi, Tian Lian Huang, Hirokazu Takahashi, et al. 2017. “The Cold-Induced Lipokine 12,13-diHOME Promotes Fatty Acid Transport into Brown Adipose Tissue.” Nature Medicine (March 27). doi:10.1038/nm.4297.

Published version

https://doi.org/10.1038/nm.4297

Link

http://nrs.harvard.edu/urn-3:HUL.InstRepos:32072310

Terms of use

This article was downloaded from Harvard University’s DASH repository, and is made available under the terms and conditions applicable to Open Access Policy Articles (OAP), as set forth at https://harvardwiki.atlassian.net/wiki/external/NGY5NDE4ZjgzNTc5NDQzMGIzZWZhMGFlOWI2M2EwYTg

Accessibility

https://accessibility.huit.harvard.edu/digital-accessibility-policy

Share Your Story

The Harvard community has made this article openly available. Please share how this access benefits you. Submit a story

Nature Medicine Letter

The lipid 12,13-diHOME acts as cold induced lipokine in mice and humans to promote fatty acid transport into brown adipose tissue

[1]Matthew D. Lynes, [1]Luiz O. Leiria, [1,2]Morten Lundh, [3]Alexander Bartelt, [1]Farnaz Shamsi, [1]Tian Lian Huang, [1]Hirokazu Takahashi, [1]Michael F. Hirshman, [3]Christian Schlein, [3]Alexandra Lee, [4]Lisa A. Baer, [4]Francis J. May, [5]Fei Gao, [5]Niven R. Narain, [5]Emily Y. Chen, [5]Michael A. Kiebish, [6]Aaron M. Cypess, [7]Matthias Blüher, [1]Laurie J. Goodyear, [3]Gökhan S. Hotamisligil, [4]Kristin I. Stanford, [1,8]Yu-Hua Tseng

[1]Section on Integrative Physiology and Metabolism, Joslin Diabetes Center, Harvard Medical School, Boston, MA, USA;
[2]The Novo Nordisk Foundation Center for Basic Metabolic Research, University of Copenhagen, Denmark
[3]Department of Genetics and Complex Diseases & Sabri Ülker Center, Harvard T.H. Chan School of Public Health, Boston, MA, USA;
[4]Department of Physiology and Cell Biology, Dorothy M. Davis Heart and Lung Research Institute, The Ohio State University, Columbus, Ohio, USA;
[5]BERG, Framingham, MA, USA;
[6]National Institutes of Health, Bethesda, MD, USA;
[7]Department of Medicine, University of Leipzig, Leipzig, Germany;
[8]Harvard Stem Cell Institute, Harvard University, Cambridge, MA, USA

Keywords: Brown adipose tissue, thermogenesis, lipokine

Corresponding author:
Yu-Hua Tseng, Ph.D.
Joslin Diabetes Center
One Joslin Place
Boston, MA 02215
Phone: 617-309-1967
Fax: 617-309-2650
E-mail: yu-hua.tseng@joslin.harvard.edu

MAIN TEXT

INTRODUCTORY PARAGRAPH (200 WORDS MAX)

Brown adipose tissue (BAT) and beige adipose tissue combust fuels for heat production in adult humans, constituting an appealing target for treatment of metabolic disorders such as obesity, diabetes, and hyperlipidemia[1,2]. Cold exposure can improve nutrient metabolism and enhance energy expenditure by activating BAT[3-5]. These therapies, however, are time consuming and uncomfortable, increasing the need for pharmacological interventions. Recently, lipids called "lipokines" with signaling properties promoting insulin sensitivity and glucose tolerance have been identified[6-8]. As BAT is a specialized lipid metabolic tissue linked to systemic metabolic homeostasis, we hypothesized that there may be thermogenic lipokines that activate BAT in response to cold. Here we show the lipid 12,13-dihydroxy-9Z-octadecenoic acid (12,13-diHOME) is an indicator and stimulator of BAT activity that negatively correlates with body mass index and insulin sensitivity. Using a global lipidomic analysis, we found 12,13-diHOME was increased in the circulation of cold challenged humans and mice and the enzymes that produce 12,13-diHOME were uniquely induced in BAT by cold. 12,13-diHOME acutely activated BAT fuel uptake and enhanced cold tolerance, resulting in decreased serum triglycerides. Mechanistically, 12,13-diHOME increased fatty acid (FA) uptake into brown adipocytes by promoting translocation of FA transporters FATP1 and CD36 to the cell membrane. In summary, our results identify a novel mechanism of BAT activation through a lipokine produced in response to cold. These data suggest novel therapeutic pathways for the treatment of metabolic disorders by mimicking cold.

BODY (1500 WORDS MAX)

Cold exposure activates substrate uptake and utilization in BAT in as little as one hour in humans[9]. We hypothesized that thermogenic lipokines linked to BAT activation might increase in subjects exposed to a cold challenge as lipokines can have effects on improving metabolism similar to cold exposure[10]. To test this hypothesis, we used liquid chromatography tandem mass spectrometry (LC-MS/MS) to measure the concentrations of a panel of 88 lipids with annotated signaling properties in the plasma of human volunteers exposed to cold[9] (Supplementary Fig. 1a,1b Supplementary Table 1). This approach to identify putative lipokines is highly sensitive and covered a broad range of oxidized fatty acid metabolites. Notably, 3 species were significantly increased by cold in human circulation after 1 hour of cold challenge ($p<0.05$, Fig. 1a, Supplementary Fig. 2).

The lipid 12,13-diHOME, however, was the only species that increased in all subjects measured (Fig. 1b) and 12,13-diHOME concentration correlated to BAT activity measured by radiolabeled glucose uptake (Fig. 1c). BAT activity and mass are both decreased with obesity[1], so to determine if 12,13-diHOME links to human obesity and its related metabolic disorders, we measured 12,13-diHOME in a cohort of 55 lean, overweight, and obese human subjects at room temperature. Importantly, we found significant negative associations between plasma concentration of 12,13-diHOME and body mass index (BMI), insulin resistance (measured by HOMA-IR), fasting plasma insulin and glucose concentrations (Fig. 1d-e and Supplementary Fig 3b-c, 3j), although the correlation with hemoglobin A1c and c-reactive peptide was not as strong (Supplementary Fig. 3d, 3e). Consistent with BMI, circulating triglycerides and leptin were also negatively correlated with plasma 12,13-diHOME (Fig. 1f and Supplementary Fig. 3f). Notably, circulating triglycerides remained significantly correlated to 12,13-diHOME after we accounted for BMI as a covariate in a linear model ($p=0.0463$, Supplementary Table 1). Circulating markers of liver function, such as alanine transaminase (ALAT) (Fig. 1g), aspartate transaminase (ASAT) (Supplementary Fig. 3h), and gamma-glutamyl transpeptidase (gGT) (Supplementary Fig. 3i), were inversely correlated with 12,13-diHOME concentration and both ALAT and ASAT remained significantly correlated when BMI was accounted as a covariate ($p=0.0494$, $p=0.0274$ respectively). Cholesterol, on the other hand, did not correlate with circulating 12,13-diHOME (Fig. 1h-l and Supplementary Fig. 3g). In this particular cohort of subjects, we found that circulating 12,13-diHOME had no association with age, gender or diabetes (Supplementary Fig. 3a, 3k-l). .

To allow in-depth mechanistic studies, we established a cold exposure model using mice housed at either 30 °C thermoneutrality (minimal BAT activity) or 4 °C (maximal BAT activity) for various durations. Consistent with what was observed in humans, exposing mice to 4°C for 1 hour increased circulating 12,13-diHOME (Fig. 2a). Of note, treatment of mice with norepinephrine (NE) for 30 minutes, which mimics sympathetic activation, also induced 12,13-diHOME production, suggesting that 12,13-diHOME is a potential product induced by both cold and sympathetic activation. Similar to acute cold challenge, one week of cold exposure also induced a pronounced increase in circulating 12,13-diHOME in male mice (Fig. 2b). In female mice, 12,13-diHOME was not significantly changed in circulation after one week of cold exposure, however, this increase did reach statistical significance after exposed to cold for 11 days (Fig. 2b,

Supplementary Fig. 4a), which may be related to the reported sexual dimorphism of lipid profiles in mouse BAT[11].

12,13-diHOME was originally identified in mice as a component of the neutrophil oxidative burst,[12] but has not been previously linked to cold or BAT biology. Biosynthesis of 12,13-diHOME and its isomer 9,10-diHOME begins via formation of 12,13- or 9,10-epOME epoxides from linoleic acid by Cytochrome P450 (Cyp) oxidases, followed by hydrolysis catalyzed by soluble epoxide hydrolases (sEH) to form the diols 12,13-diHOME and 9,10-diHOME (Fig. 2c). Among the four sEH genes, *Ephx1* and *Ephx2* are the major isoforms expressed in adipose tissue[13] and although *Ephx2* null mice have decreased blood pressure[14], thermogenic function has not been reported in Ephx1[15] or *Ephx2* knockout mice. We found that acute cold exposure (i.e., 1 hour) induced a nearly 14-fold increase of Ephx2 in BAT (Fig. 2d). Chronic cold (e.g., 1 week) also increased both *Ephx1* (Fig. 2e) and *Ephx2* (Fig. 2f) expression only in BAT but not other tissues where sEH is expressed (Supplementary Fig. 4b). Meta-analysis of publically available datasets profiling gene expression in BAT from mice exposed to cold for different periods of time also consistently showed increased *Ephx* expression and differential regulation of several *Cyp* genes that may participate in this pathway[16-18] in BAT (Supplementary Fig. 4c). We detected a high concentration of 12,13-diHOME in adipose tissue (Supplementary Fig 4d), and *ex vivo* experiments showed that 12,13-diHOME secretion from BAT is higher than WAT (Fig. 2g).

To further investigate whether BAT or WAT could be a source of 12,13-diHOME upon cold exposure, we used LC-MS/MS to measure 12,13-diHOME in adipose from wild-type and *Myf5*^{cre}*BMPr1a*$^{f/f}$ mice, which display a severe defect in classical BAT development and a compensatory browning of sWAT[19]. Cold exposure increased 12,13-diHOME concentration in BAT from wild-type mice, yet this effect was severely impaired in BAT from the *Myf5*^{cre}*BMPr1a*$^{f/f}$ mice (Fig. 2h). These data strongly suggest that BAT is a major source of increased circulating 12,13-diHOME after cold exposure, although circulating 12,13-diHOME in *Myf5*^{cre}*BMPr1a*$^{f/f}$ mice is not different from control animals (Supplementary Fig. 4a), raising the possibility that beige adipocytes recruited in sWAT tissue of the *Myf5*^{cre}*BMPr1a*$^{f/f}$ mice might also be a potential source. Concordant with these data, 12,13-diHOME was elevated in sWAT from cold challenged male *Myf5*^{cre}*BMPr1a*$^{f/f}$ mice with enhanced beige adipogenesis compared to wild-type mice housed in cold for two days, while no effect was observed after 11 days in female mice (Supplementary Fig. 4e). Pharmacologic BAT activation using daily treatment with the

β3-adrenergic agonist CL316,243 for 10 days increased *Ephx2* expression in BAT and *Ephx1* expression in sWAT (Supplementary Fig. 4f, 4g), suggesting that 12,13-diHOME can be produced by brown or beige fat in response to β3-adrenergic stimulation. One challenge to understanding the flux of 12,13-diHOME *in vivo* is that this lipid can be both consumed in the diet and produced in the body, so further characterization of the biosynthetic pathway will require labeling 12,13-diHOME itself and warrants future studies.

To test our initial hypothesis that putative lipokines induced by cold can facilitate increased thermogenesis, we treated mice with either 12,13-diHOME and measured core body temperature during an acute cold challenge. To minimize cytotoxic effects, we chose to use the dosage of 1 μg/kg with a target concentration of 30-50 nM for *in vivo* administration to mimic the physiologic concentration after cold exposure. This dose is based on the measured circulating concentration of 12,13-diHOME at room temperature and after cold exposure, and is orders of magnitude lower than the reported concentration that causes lung mitochondrial dysfunction[20]. Importantly, treatment with 12,13-diHOME protected mice from the decrease in body temperature during cold challenge compared to both vehicle-treated mice and mice injected with the precursor lipid 12,13-epOME (Fig. 3a). Of note, except for a very transient increase in diastolic pressure, 12,13-diHOME had no effect on blood pressure and pulse (Supplementary Fig. 5a, 5b, 5c), suggesting that 12,13-diHOME possesses a therapeutic benefit over sympathomimetics for BAT activation by avoiding potential side effects[21], such as tachycardia or hypertension. Consistent with these findings, 12,13-diHOME-treated animals displayed increased oxygen consumption and carbon dioxide production in the cold (Fig. 3b). These changes result in a decreased respiratory exchange ratio (Fig. 3c), indicating increased lipid oxidation and further suggesting the effect of 12,13-diHOME on BAT metabolism is mediated, at least in part, through enhanced lipid metabolism.

To test therapeutic applications of 12,13-diHOME, we treated diet-induced obese mice with 12,13-diHOME daily for 2 weeks at 10 μg/kg body weight. Although no effect on body weight, glucose tolerance, or circulating non-esterified FA (Supplementary Fig. 6a, 6b, 6c) were observed at this dose, 12,13-diHOME decreased circulating triglycerides (Fig. 3d) and increased expression of lipoprotein lipase (*LPL*) in BAT, suggesting increased hydrolysis of triglycerides[22,23] (Supplementary Fig. 6d). These results, together with well-supported reports that activated BAT takes up large quantities of FA from circulating triglyceride-rich lipoproteins[23-27], led us to test the effects of 12,13-

diHOME on lipid uptake *in vivo*. Since 12,13-diHOME decreased circulating triglycerides and the principal source of FA *in vivo* is in the form of triglycerides packaged into lipoproteins, we measured the effect of 12,13-diHOME on the uptake of radiolabeled triglycerides delivered by oral gavage (Fig. 3e). Indeed, mice treated with 12,13-diHOME exhibited increased BAT specific lipid uptake and improved oral lipid tolerance (Supplementary Fig. 6e). Similarly, 12,13-diHOME increased radiolabeled FA uptake (Fig. 3f) and glucose uptake (Supplementary Fig. 6f) specifically into BAT, similar to a level achieved by NE stimulation.

Given the fast and dynamic nature of FA uptake, we sought to monitor 12,13-diHOME-stimulated fatty acid uptake in real time. We generated transgenic mice expressing firefly luciferase specifically in brown adipocytes (UCP1cre$^{+/-}$Rosa(stop)Luc$^{+/-}$). We injected these mice intravenously with FFA-SS-Luc, a fatty acid-luciferin conjugate that follows the uptake of natural FA and releases luciferin only after internalization[28]. In this model, luciferase is exclusively expressed in UCP1-expressing adipocytes, so the luciferin substrate can only be oxidized in these cells to release light to measure brown adipocyte FA uptake (Fig. 3g, Supplementary Video 1). Mice treated with 12,13-diHOME had an increased luminescent signal in BAT compared to vehicle-treated animals that was both rapid and sustained over the course of the experiment (Fig. 3h, 3i). Taken together, these data demonstrate a pro-thermogenic effect of 12,13-diHOME that is linked to acute BAT-specific FA uptake.

To identify potential cell autonomous mechanisms for increased FA uptake in BAT, we tested the effects of 12,13-diHOME on brown adipocytes constitutively expressing luciferase *in vitro*. In agreement with experiments *in vivo*, FFA-SS-Luc uptake *in vitro* was also increased (Fig. 4a, Supplementary Video 2), while no additive effect of NE treatment was observed (data not shown), suggesting 12,13-diHOME might act downstream of NE. Similarly, 12,13-diHOME markedly increased radiolabeled FA uptake in brown adipocytes with an increase FA oxidation that did not reach statistical significance (Fig. 4b, 4c). As a result of consuming the FA fuel, basal respiration was increased in 12,13-diHOME treated brown adipocytes (Fig. 4d), but there was no effect on maximal respiratory capacity or uncoupling Together with the in vivo data (Fig. 3b, 3c), these findings indicates that the effect of 12,13-diHOME was primarily to increase metabolic flux and fuel consumption. In adipocytes, FA uptake is mediated in part by a diverse family of fatty acid transport proteins including CD36 and FATP1, both of which are hormone-sensitive FA transporters[26,29] required for non-shivering thermogenesis in

mice[30,31]. Membrane translocation of both the low glycosylation form of CD36[26] and oligomeric FATP1[32] are robustly induced by 12,13-diHOME, consistent with increased fatty acid uptake (Fig. 4e, 4f, 4g, Supplementary Fig. 7). Fractionation of cellular compartments was confirmed using Tubulin as a marker of cytosol and Cadherin to mark the membrane.

Taken together, these results lead us to propose a model (Fig. 4h), wherein cold exposure activates production of 12,13-diHOME in BAT tissue by increasing lipolysis to provide substrates for sEH and increasing sEH gene expression, ultimately leading to increased circulating 12,13-diHOME. 12,13-diHOME acts, at least in part, via an autocrine/paracrine mechanism to activate fatty acid transporter translocation in brown adipocytes leading to increased FA uptake and triglyceride clearance, facilitating thermogenesis by providing fuel. Chronic cold exposure further increases gene expression of sEH, specifically in brown or beige adipocytes, to increase biosynthesis of 12,13-diHOME. Notably, even metabolically inert fatty acids are known to directly activate UCP1[33], and the direct effects of 12,13-diHOME on UCP1-mediated uncoupling require further investigation. Our *in vivo* experiments, however, supported a direct effect of 12,13-diHOME on FA uptake.

Based on our model, 12,13-diHOME facilitates BAT thermogenic activity by selectively promoting fuel uptake, suggesting potential applications for treating hyperlipidemia. Indeed, acute 12,13-diHOME treatment protected mice from cold challenge, and chronic treatment (i.e., one week) of obese mice with 12,13-diHOME resulted in a reduction of circulating triglyceride without alteration of body weight. These data point out a complex fuel consumption and refueling process that impact energy balance during cold exposure and presumably upon 12,13-diHOME treatment. In cold conditions, fatty acids in brown adipocytes serve as both fuels to be oxidized for thermoregulation, as well as substrates for biosynthesis of 12,13-diHOME. Since 12,13-diHOME activates fatty acid uptake, consumption of cellular fuel is coupled to a potent and specific refueling signal. By identifying this mechanism of BAT specific lipid utilization, it may be possible to unlock the maximum therapeutic potential of brown fat in humans.

ACKNOWLEDGEMENTS

This work was supported in part by US National Institutes of Health (NIH) grants R01DK077097 (to Y.-H.T.), K01-DK-105109 (to K.I.S.), R01-DK-099511 (to L.J.G.) and

P30DK036836 (to Joslin Diabetes Center's Diabetes Research Center, DRC) from the National Institute of Diabetes and Digestive and Kidney Diseases, a research grant from the American Diabetes Foundation (ADA 7-12-BS-191, to Y.-H.T.) and by funding from the Harvard Stem Cell Institute (to Y.-H.T.). M.D.L was supported by NIH fellowships (T32DK007260 and F32DK102320). A.B. was supported by a Deutsche Forschungsgemeinschaft Research Fellowship (BA 4925/1-1). M.L was supported by the Danish Council for Independent Research. We thank K. Longval and A. Clermont of the Joslin Diabetes Center Physiology core, H. Rockwell, K. Schlosser and J. McDaniel at BERG and P. Lizotte for expert technical assistance. We thank Karen Inouye for critical discussion. We acknowledge P. Soriano (Mount Sinai School of Medicine, New York, NY) for providing *Myf5*-cre mice. We apologize to colleagues whose work we could not cite due to space limitations.

AUTHOR CONTRIBUTIONS

M.D.L. designed research, carried out experiments, analyzed data and wrote the paper. L.O.L. carried out *in vitro* fatty acid uptake and Seahorse assays. M.L. carried out translocation assays. A.B., A.L. and C.S. carried out *in vivo* fatty acid, triglyceride and glucose uptake assays. F.S. and T.L.H. performed gene expression analysis and immunoblotting. H.T. carried out *in vitro* fatty acid uptake assays. M.F.H., L.A.B. and F.J.M. carried out *in vivo* experiments. F.G., N.R.N. and M.A.K. oversaw lipidomics experiments. E.Y.C. performed lipidomic experiments and analyzed data. A.M.C. designed research and carried out human cold exposure experiments. M.B. provided human plasma from well-phenotyped human individuals for 12,13-diHOME measurements. L.J.G. oversaw fatty acid uptake experiments. G.S.H. oversaw *in vivo* tracer uptake experiments. K.I.S. oversaw *in vivo* experiments and analyzed data. M.D.L. and Y.-H.T. directed the research and co-wrote the paper.

CONFLICT OF INTEREST STATEMENT

The authors declare no conflicts of interest.

MAIN TEXT REFERENCE

1. Townsend, K.L. & Tseng, Y.H. Brown adipose tissue: recent insights into development, metabolic function, and therapeutic potential. *Adipocyte* **1**, 13-24 (2012).

2. Lynes, M.D. & Tseng, Y.H. Unwiring the transcriptional heat circuit. *Proc Natl Acad Sci U. S A* **111**, 14318-14319 (2014).
3. Romu, T.*, et al.* A randomized trial of cold-exposure on energy expenditure and supraclavicular brown adipose tissue volume in humans. *Metabolism* **65**, 926-934 (2016).
4. Schellen, L., Loomans, M.G., de Wit, M.H., Olesen, B.W. & van Marken Lichtenbelt, W.D. The influence of local effects on thermal sensation under non-uniform environmental conditions--gender differences in thermophysiology, thermal comfort and productivity during convective and radiant cooling. *Physiol Behav* **107**, 252-261 (2012).
5. Hanssen, M.J.*, et al.* Short-term cold acclimation improves insulin sensitivity in patients with type 2 diabetes mellitus. *Nat. Med* **21**, 863-865 (2015).
6. Cao, H.*, et al.* Identification of a lipokine, a lipid hormone linking adipose tissue to systemic metabolism. *Cell* **134**, 933-944 (2008).
7. Liu, S.*, et al.* A diurnal serum lipid integrates hepatic lipogenesis and peripheral fatty acid use. *Nature* **502**, 550-554 (2013).
8. Yore, M.M.*, et al.* Discovery of a class of endogenous mammalian lipids with anti-diabetic and anti-inflammatory effects. *Cell* **159**, 318-332 (2014).
9. Cypess, A.M.*, et al.* Cold but not sympathomimetics activates human brown adipose tissue in vivo. *Proc. Natl. Acad Sci. U. S. A* **109**, 10001-10005 (2012).
10. Oh, D.Y.*, et al.* GPR120 is an omega-3 fatty acid receptor mediating potent anti-inflammatory and insulin-sensitizing effects. *Cell* **142**, 687-698 (2010).
11. Hoene, M.*, et al.* The lipid profile of brown adipose tissue is sex-specific in mice. *Biochim. Biophys. Acta* **1842**, 1563-1570 (2014).
12. Thompson, D.A. & Hammock, B.D. Dihydroxyoctadecamonoenoate esters inhibit the neutrophil respiratory burst. *J Biosci* **32**, 279-291 (2007).
13. Su, A.I.*, et al.* A gene atlas of the mouse and human protein-encoding transcriptomes. *Proc Natl. Acad Sci U S. A* **101**, 6062-6067 (2004).
14. Sinal, C.J.*, et al.* Targeted disruption of soluble epoxide hydrolase reveals a role in blood pressure regulation. *J Biol Chem* **275**, 40504-40510 (2000).
15. Miyata, M.*, et al.* Targeted disruption of the microsomal epoxide hydrolase gene. Microsomal epoxide hydrolase is required for the carcinogenic activity of 7,12-dimethylbenz[a]anthracene. *J Biol Chem* **274**, 23963-23968 (1999).
16. Marcher, A.B.*, et al.* RNA-Seq and Mass-Spectrometry-Based Lipidomics Reveal Extensive Changes of Glycerolipid Pathways in Brown Adipose Tissue in Response to Cold. *Cell Rep* **13**, 2000-2013 (2015).
17. Hao, Q.*, et al.* Transcriptome profiling of brown adipose tissue during cold exposure reveals extensive regulation of glucose metabolism. *Am J Physiol Endocrinol Metab* **308**, E380-392 (2015).
18. Rosell, M.*, et al.* Brown and white adipose tissues: intrinsic differences in gene expression and response to cold exposure in mice. *Am J Physiol Endocrinol Metab* **306**, E945-964 (2014).
19. Schulz, T.J.*, et al.* Brown-fat paucity due to impaired BMP signalling induces compensatory browning of white fat. *Nature* **495**, 379-383 (2013).
20. Sisemore, M.F.*, et al.* Cellular characterization of leukotoxin diol-induced mitochondrial dysfunction. *Arch Biochem Biophys* **392**, 32-37 (2001).

21. Redman, L.M.*, et al.* Lack of an effect of a novel beta3-adrenoceptor agonist, TAK-677, on energy metabolism in obese individuals: a double-blind, placebo-controlled randomized study. *Journal of Clinical Endocrinology & Metabolism* **92**, 527-531 (2007).
22. Klingenspor, M.*, et al.* Multiple regulatory steps are involved in the control of lipoprotein lipase activity in brown adipose tissue. *J Lipid Res* **37**, 1685-1695 (1996).
23. Bartelt, A.*, et al.* Brown adipose tissue activity controls triglyceride clearance. *Nat. Med* **17**, 200-205 (2011).
24. Berbee, J.F.*, et al.* Brown fat activation reduces hypercholesterolaemia and protects from atherosclerosis development. *Nature communications* **6**, 6356 (2015).
25. Khedoe, P.P.*, et al.* Brown adipose tissue takes up plasma triglycerides mostly after lipolysis. *J Lipid Res* **56**, 51-59 (2015).
26. Schlein, C.*, et al.* FGF21 Lowers Plasma Triglycerides by Accelerating Lipoprotein Catabolism in White and Brown Adipose Tissues. *Cell Metab* **23**, 441-453 (2016).
27. Warner, A.*, et al.* Activation of beta3-adrenoceptors increases in vivo free fatty acid uptake and utilization in brown but not white fat depots in high-fat fed rats. *Am J Physiol Endocrinol Metab*, ajpendo.00204.02016 (2016).
28. Henkin, A.H.*, et al.* Real-time noninvasive imaging of fatty acid uptake in vivo. *ACS Chem Biol* **7**, 1884-1891 (2012).
29. Stahl, A., Evans, J.G., Pattel, S., Hirsch, D. & Lodish, H.F. Insulin causes fatty acid transport protein translocation and enhanced fatty acid uptake in adipocytes. *Dev. Cell* **2**, 477-488 (2002).
30. Wu, Q.*, et al.* Fatty acid transport protein 1 is required for nonshivering thermogenesis in brown adipose tissue. *Diabetes* **55**, 3229-3237 (2006).
31. Putri, M.*, et al.* CD36 is indispensable for thermogenesis under conditions of fasting and cold stress. *Biochem Biophys Res Commun* **457**, 520-525 (2015).
32. Richards, M.R.*, et al.* Oligomerization of the murine fatty acid transport protein 1. *J Biol Chem* **278**, 10477-10483 (2003).
33. Shabalina, I.G., Kalinovich, A.V., Cannon, B. & Nedergaard, J. Metabolically inert perfluorinated fatty acids directly activate uncoupling protein 1 in brown-fat mitochondria. *Archives of toxicology* **90**, 1117-1128 (2016).

MAIN FIGURE LEGENDS

Figure 1. Discovery of 12,13-diHOME, a cold-induced lipokine linked to BAT activation. (a) Volcano plot of 88 lipids comparing the fold induction after cold challenge to the p value (paired t-test). The dashed line indicates a p value of 0.05. 12,13-diHOME is highlighted in red. n=9 individual subjects. (b) Individual plasma concentration of 12,13-diHOME before and after cold challenge. The p-value for a paired t-test is shown. (c) Plasma 12,13-diHOME concentration plotted with BAT specific activity as measured by positron emission tomography (PET) scan of radiolabeled fluorodeoxyglucose. R is the

Spearman correlation between 12,13-diHOME and BAT activity. (d-i) Circulating 12,13-diHOME concentration plotted against body mass index (BMI) (d), HOMA-IR (e), circulating triglycerides (f), circulating alanine transaminase (ALAT) (g), circulating HDL-cholesterol (h), and LDL-cholesterol (i). In each panel, R is the Spearman correlation between 12,13-diHOME and each circulating parameter. In each panel males are shown in blue while females are shown in pink. N=55 individual subjects (13M/42F). The p value shown was calculated using algorithm AS 89.

Figure 2. The biosynthetic pathway of 12,13-diHOME is selectively increased in BAT with cold in mice. (a) Serum 12,13-diHOME concentration in control mice compared to mice treated with Norepinephrine (NE) for 30 minutes and mice exposed to 4°C cold for 1 hour. Data are means +/- s.e.m.; n= 6 control mice, 7 NE treated, 7 cold exposed. *p<0.05, *p<0.005 by t-test. (b) Serum concentration of 12,13-diHOME in male and female mice after a 7 day cold challenge vs. mice housed at thermoneutrality. Data are means +/- s.e.m.; n= 6 mice per group; *p<0.05 by t-test. (c) Biosynthetic pathway of 12,13-diHOME production. (d) *Ephx1* and *Ephx2* mRNA expression measured by qPCR in BAT from control mice vs. mice exposed to 4°C cold for 1 hour. Data are means +/- s.e.m.; n= 6 control mice, 7 cold exposed. *p<0.05 by t-test. (e) *Ephx1* gene expression measured by qPCR in BAT, sWAT, and eWAT from mice housed at thermoneutrality or cold for 7 days. Data are presented as normalized means ± s.e.m.; n=4 per group; *p<0.05 by t-test. (f) *Ephx2* gene expression measured by qPCR in BAT, sWAT, and eWAT of mice housed at either thermoneutrality or cold for 7 days. Data are presented as normalized means ± s.e.m.; n=4 per group; *p<0.05 by t-test. (g) 12,13-diHOME concentration in media from BAT and sWAT cultured *ex vivo* for 1 hour normalized to tissue weight. Data are means +/- s.e.m.; n= 6 mice; *p<0.05 by t-test. (h) 12,13-diHOME concentrations in BAT from wild type and *Myf5*^{cre}*BMPr1a*$^{f/f}$ mice housed at cold or thermoneutrality for 2 or 11 days. Data are plotted as the normalized means ± s.e.m.; n=5 WT thermoneutral males, 5 WT cold males, 4 *Myf5*^{cre}*BMPr1a*$^{f/f}$ thermoneutral males, 5 *Myf5*^{cre}*BMPr1a*$^{f/f}$ cold males, 3 WT thermoneutral females, 6 WT cold females, 4 *Myf5*^{cre}*BMPr1a*$^{f/f}$ thermoneutral females, 6 *Myf5*^{cre}*BMPr1a*$^{f/f}$ cold females; *p<0.05 by t-test.

Figure 3. 12,13-diHOME enhances cold tolerance and facilitate fatty acid uptake into BAT. (a) Body temperature in mice cold challenged at 4°C for 90 min after pretreatment

with 12,13-diHOME, 12,13-epOME or vehicle. Data are means ± s.e.m.; n=5 per group; *p<0.05 12,13-diHOME vs. Vehicle by ANOVA with post-hoc Bonferroni test. (b and c) Total V(O_2) consumed and V(CO_2) produced (b) and average respiratory exchange ratio (R.E.R., c) measurements measured by CLAMS for 1 h at cold (4°C) in mice acutely treated with 12,13-diHOME or vehicle. (d) Serum triglycerides in mice fed HFD and treated with 12,13-diHOME or vehicle for 2 weeks. Data are means +/- s.e.m.; n=6 treated vs. 5 controls; *p<0.05 by t-test. (e) Radioactivity per 10 mg of liver, gastrocnemius muscle (Gastroc), soleus muscle, heart, BAT, sWAT and epididymal white adipose tissue (eWAT) from mice treated with vehicle or 12,13-diHOME and then given an oral bolus of ^{3}H-labeled triglyceride. Data are means ± s.e.m.; n=6 per group; *p<0.05 by t-test. (f) Radioactivity per 10 mg of tissues from mice treated with vehicle, Norepinephrine (NE) or 12,13-diHOME and then given a bolus of ^{3}H-labeled oleate. Data are means ± s.e.m.; n=8 per group; *p<0.05 12,13-diHOME vs. Vehicle by ANOVA with post-hoc Bonferroni test. (g) Representative images of luciferase activity in UCP1cre$^{+/-}$ Rosa(stop)Luc$^{+/-}$ injected intravenously with luciferin-conjugated fatty acid and 12,13-diHOME or vehicle. Data are representative images at 0, 10 and 55 min. (h) Quantification of luciferase activity in (g). (i) Total luciferase counts from 6 individual experiments were averaged plotted as the normalized means ± s.e.m.; n=6 per group; *p<0.05 12,13-diHOME vs. vehicle by t-test.

Figure 4. 12,13-diHOME promotes fatty acid uptake *in vitro* by activating the translocation and oligomerization of FA transporters. (a) Fatty acid uptake in mature brown adipocytes constitutively expressing firefly luciferase that were pretreated with either 12,13-diHOME or vehicle measured by luciferase activity using 10 μM FFA-SS-Luc. Data are plotted as the normalized means ± s.e.m.; n=6 wells per group; *p<0.05 12,13-diHOME vs. vehicle by ANOVA with post-hoc Bonferroni test. (b) Radiolabeled ^{14}C palmitic acid uptake in mature brown adipocytes pretreated for 15 minutes with either 12,13-diHOME or vehicle. The data was normalized by protein content. Data are presented as means ± s.e.m.; n=10-11 wells per group; *p<0.05 12,13-diHOME vs. vehicle by t-test. (c) Radiolabeled ^{14}C palmitic acid oxidation in mature brown adipocytes pretreated with either 12,13-diHOME or vehicle. The data was normalized by protein content. Data are presented as means ± s.e.m.; n=10-11 wells per group; p value is shown for 12,13-diHOME vs. vehicle by t-test. (d) Basal respiration of mature brown adipocytes treated with either 12,13-diHOME or vehicle. The data was normalized by

protein content. Data are presented as means ± s.e.m.; n=10-11 wells per group; *p<0.05 12,13-diHOME vs. vehicle by t-test. (e) Western blot analysis of membrane and cytosol fractions of differentiated WT-1 brown adipocytes treated with 12,13-diHOME or vehicle. Data are presented as a representative image; n=3 separate experiments. (f) The upper band corresponding to the oligomer form of FATP1 was measured by densitometry from immunoblots of three independent experiments. Data are presented as means ± s.e.m.; n=3 separate experiments; *p<0.05 12,13-diHOME vs. vehicle by 1-way ANOVA. (g) Densitometry of the low glycosylation form of CD36 from immunoblots of three independent experiments. Data are presented as means ± s.e.m.; n=3 separate experiments; *p<0.05 12,13-diHOME vs. vehicle by 1-way ANOVA. (h) Proposed model of 12,13-diHOME biosynthesis and action in cold activated BAT.

ONLINE METHODS

General experimental approaches

No samples, mice, human subjects or data points were excluded from the reported analyses. Samples were not randomized to experimental groups. Analyses were not performed in a blinded fashion except as noted below.

Human Subjects

Human plasma was acquired from a previously performed cold exposure experiment approved by the Human Studies Institutional Review Boards of Beth Israel Deaconess Medical Center[9]. All subjects gave written informed consent before taking part in the study. Briefly, 9 healthy volunteers participated in 3 separate, independent study visits conducted in random order based on a Latin Square design. The night before the study day, the subjects were admitted to the clinical research center and began fasting from 12:00 AM onward. Room temperature was maintained above 23 °C throughout the stay in the clinical research center. Upon waking the next morning, the volunteers put on a standard hospital scrub suit. Depending on the study day, one of three stimuli was given: a single intramuscular dose of ephedrine 1 mg/kg; an equal volume of saline; or the volunteer was transported to a room set to 20 °C and donned a surgeon's cooling vest (Polar Products) with the water temperature set to 14 °C that was monitored by a digital thermometer (Fisher Scientific). Sixty minutes after the injection of ephedrine, saline, or the initiation of cold exposure, blood was drawn for measurement of lipid levels, and then an intravenous bolus of 440 MBq (12 mCi) of ^{18}F-FDG was

administered. 60 min after the ^{18}F-FDG injection, images were acquired using a Discovery LS multidetector helical PET-CT scanner (GE Medical Systems). BAT mass and activity were both quantified using the PET-CT Viewer shareware.

For the second cohort of human subjects, 55 individuals were selected from the Leipzig biobank (42 women, 13 men) to represent a wide range of body mass index (BMI: 17.5 – 75.4 kg/m²), categories of lean (BMI<25kg/m²; n=15; 4 M/11 F), overweight (BMI 25.1-29.9kg/m²; n=13; 4 M/9 F) or obese (BMI>30kg/m²; n=27; 5 M/22 F) and glucose metabolism parameters (fasting plasma glucose 3.9 – 13.4 mmol/l; fasting plasma insulin 3.8 – 451 pmol/l, HOMA-IR: 0.1 - 25). In the subgroup of lean, all individuals were normal glucose tolerant (NGT), whereas in the overweight subgroup, 10 individuals with NGT and 3 with type 2 diabetes (T2D) and in the obese group 20 NGT and 7 T2D subjects were included. Phenotyping, definition of NGT and T2D, as well as analyses of serum/plasma parameters (fasting plasma insulin (FPI), fasting plasma glucose (FPG), hemoglobin A1c (HbA1c), C-reactive protein (CrP), leptin, total cholesterol, aspartate transaminase (ASAT), and gamma-glutamyl transpeptidase (gGT) serum concentrations) were performed as described previously[35]. The collection of human biomaterial, serum analyses and phenotyping were approved by ethics committee of the University of Leipzig (approval numbers: 159-12-21052012 and 017-12-23012012) and all subjects gave written informed consent before taking part in the study.

Lipidomic profiling and 12,13-diHOME quantification

All lipid standards were purchased from Cayman Chemical Company, Avanti Polar Lipids, or Santa Cruz Biotechnology, Inc. C_{18}SPE cartridges were purchased from Biotage. All solvents are of HPLC or LC-MS/MS grade and were acquired from Sigma-Aldrich, Fisher Scientific, or VWR International. Tissue samples were homogenized in 0.1x PBS in Omni homogenizing tubes with ceramic beads at 4^{o}C. Aliquots of 100 µL serum or 1mg protein of homogenized tissue (measured by BCA) were taken, depending on the experiment. A mixture of deuterium-labeled internal standards was added to each aliquot, followed by 3x volume of sample of cold methanol (MeOH). Samples were vortexed for 5 min and stored at −20 °C overnight. Cold samples were centrifuged at 14,000g for 10 min, and the supernatant was then transferred to a new tube and 3 mL of acidified H_2O (pH 3.5) was added to each sample prior to C_{18} SPE and performed as previously described[36]. The methyl formate fractions were collected, dried under

nitrogen, and reconstituted in 50 µL MeOH:H_2O (1:1, by volume). Samples were transferred to 0.5 mL tubes and centrifuged at 20,000g at 4 °C for 10 min. Thirty-five microliters of supernatant was transferred to LC–MS/MS vials for analysis using the BERG LC–MS/MS mediator lipidomics platform. Separation of signaling lipids was performed on an Ekspert MicroLC 200 system (Eksigent Technologies) with a Synergi™ Fusion-RP capillary C_{18} column (150 × 0.5 mm, 4 µm; Phenomenex Inc.) heated to 40°C. A sample volume of 10 µL was injected at a flow rate of 20 µL/min. Lipids were separated using mobile phases A (100 % H_2O, 0.1 % acetic acid) and B (100 % MeOH, 0.1 % acetic acid) with a gradient starting at 60% B for 0.5 min, steadily increasing to 80% B by 5 min, reaching 95% B by 9 min, holding for 1 min, and then decreasing to 60% B by 12 min. MS analysis was performed on a SCIEX TripleTOF® 5600+ system using the HR-MRM strategy consisting of a TOF MS experiment looped with multiple MS/MS experiments. MS spectra were acquired in high-resolution mode (>30,000) using a 100-ms accumulation time per spectrum. Full-scan MS/MS was acquired in high sensitivity mode, with an accumulation time optimized per cycle. Collision energy was set using rolling collision energy with a spread of 15V. The identity of a component was confirmed using PeakView® software (SCIEX), and quantification was performed using MultiQuant™ software (SCIEX). The quantification of 12,13-diHOME was performed against a standard calibration curve built with 5 points ranging from 0.01pg/µL to 100pg/µL. Obtained values were corrected with the corresponding internal standard d_4-9,10-diHOME. All measurements were performed in a blinded fashion.

Mice and treatments

All animal procedures were approved by the Institutional Animal Use and Care Committee at Joslin Diabetes Center and Harvard T.H. Chan School of Public Health. The experiments were not randomized. No statistical method was used to predetermine animal's sample size. For the cold exposure experiments, radiolabeled FA uptake experiment, and diet-induced obesity experiment, 12 week old male C57BL/6J mice (Stock no. 000664) were purchased from The Jackson Laboratory. For acute BAT activation, mice were either sacrificed as control animals, treated with NE for 30 minutes, or placed at 4°C for 1 hour, then sacrificed for serum and tissue collection. In chronic cold exposures, transgenic mice carrying floxed alleles for the BMP receptor 1A were used to generate conditional gene deletions mouse models by intercrossing with *Myf5*-driven cre recombinase and compared to cre-negative littermate controls as described

previously[19]. In addition to C57BL/6J mice, these transgenic animals were used for all chronic cold exposure experiments, with mice 10-18 weeks of age housed in a temperature controlled diurnal incubator (Caron Products & Services Inc.) at either 4°C (cold) or 30°C (thermoneutrality) on a 12 hour light/dark cycle. In all experiments, interscapular BAT, inguinal sWAT, and serum were dissected after sacrifice.

For *ex vivo* tissue incubation experiments, interscapular BAT and inguinal sWAT were dissected from 12 week old male C57BL/6J mice and incubated at 37°C in Krebs solution for 1 hour, after which the tissue was discarded and LC-MS/MS was performed on the conditioned Krebs solution.

For cold tolerance assay, mice were injected retro-orbitally with 1 µg/kg body weight 12,13-diHOME in 0.1% w/v BSA in PBS or vehicle, then immediately placed in a cold room maintained at 4°C and body core temperature was determined by rectal probe measurements. Mice injected retro-orbitally were also used to measure blood pressure and pulse with the tail cuff method (Hatteras Instruments).

For *in vivo* triglyceride organ uptake studies, mice were orally gavaged with 10 mL/kg olive oil (Sigma) containing [9,10-^{3}H(N)]-triolein (PerkinElmer, 0.3 mCi/kg) 15 minutes after treatment with either vehicle, 1 µg/kg body weight 12,13-diHOME in 0.1% BSA PBS. Similarly, an oleate/^{3}H-oleate tracer mix was complexed to fatty acid-free BSA[26] and injected into the tail vein of wild type C57BL/6J mice 15 minutes after treatment with either vehicle, 1 µg/kg body weight 12,13-diHOME in 0.1% BSA PBS or NE. Glucose uptake studies were also performed by injection into the tail vein with 2-desoxy-D-[^{14}C] -glucose (PerkinElmer, 0.025 mCi per kg) in PBS 15 minutes after treatment with either vehicle, 1 µg/kg body weight 12,13-diHOME in 0.1% BSA PBS or NE. In all assays, organs were harvested after 15 minutes of radiotracer uptake under terminal anesthesia and systemic perfusion with PBS-heparin (10 U/ml) via the left heart ventricle. Tissues were homogenized by using Solvable (PerkinElmer) and disintegrations per minute per organ data were calculated by scintillation counting.

For *in vivo* bioluminescent fatty acid uptake experiments, UCP1cre$^{+/-}$ mice (Stock no. 024670) were bred with Rosa(stop)Luc$^{+/+}$ (Stock no. 005125), both obtained from The Jackson Laboratory. Male offspring carrying the UCP1-cre allele were injected retro-orbitally with 1 ug/kg body weight 12,13-diHOME in 0.1% BSA PBS or vehicle, and all mice were co-injected with 2 µm FFA-SS-Luc (Intrace Medical). Mice were anesthetized with isofluorane and imaged using the IVIS Spectrum CT using sequential 30 s

exposures for 1 hour. Data was analyzed using Living Image Software and movies were assembled from individual images using ImageJ.

For CLAMS studies, mice were injected intravenously with 1 μg/kg body weight 12,13-diHOME in 0.1% BSA PBS or vehicle and then monitored using the CLAMS system in cold conditions (4°C) for 1 hour. Respiratory exchange ratio (R.E.R.) was calculated as the ratio of total carbon dioxide produced to total oxygen consumed.

For the experiments with daily injections of 12,13-diHOME, mice were fed with a high-fat diet containing 60 kcal% fat (Research Diets Stock no. D12492) for 16 weeks prior to treatment and during the course of the experiment. Mice were first injected intraperitoneally daily with 1ug/kg body weight,13-diHOME in 0.1% BSA w/v in PBS or vehicle and body for one week, then injected every day with 10ug/kg body weight two weeks. For all experiments, serum was collected and triglycerides were measured using a standard enzymatic assay (ZenBiosystems). Non-esterified FA were also measured with a colorimetric assay (Wako Chemicals USA). High-density and low-density lipoprotein fractions were isolated and cholesterol was measured with a colorimetric assay (Abcam). All mice were allowed ad libitum access to water and food.

mRNA Expression

Total RNA was extracted from tissue with Trizol and purified using a spin column kit (Zymo Research). RNA (500 ng-1 μg) was reverse transcribed with a high-capacity complementary DNA (cDNA) reverse transcription kit (Applied Biosystems). Real-time PCR was performed in mouse tissues starting with 10 ng of cDNA and forward and reverse oligonucleotide primers (300 nM each) in a final volume of 10 μl with SYBR green PCR Master Mix (Roche). Fluorescence was determined and analyzed in an ABI Prism 7900 sequence detection system (Applied Biosystems). Acidic ribosomal phosphoprotein P0 (ARBP) expression was used to normalize gene expression. Real time PCR primer sequences are listed in Supplementary Table 3.

In vitro lipid assays

Stromal vascular cells were isolated from interscapular brown adipose tissue dissected from TgLuc mice (Stock no. 008450) obtained from The Jackson Laboratory. Cells were immortalized and differentiated into adipocytes *in vitro* according to the WT-1 protocol[34]. After 1 hour of serum starvation, mature adipocytes were treated with 1 μM 12,13-diHOME or methyl acetate vehicle in 0.1% w/v BSA in PBS for 15 minutes. After

this treatment, cells were incubated with 10 μm FFA-SS-Luc (Intrace Medical) and imaged using the IVIS Spectrum CT using sequential 30 s exposures for 1 hour. Data was analyzed using Living Image Software and movies were assembled from individual images using ImageJ. All cultures were confirmed to be Mycoplasma free.

FA uptake and oxidation were determined by measuring both ^{14}C-labeled palmitic acid uptake and conversion of ^{14}C-labeled palmitic acid into CO_2. WT-1 brown preadipocytes were differentiated according to a standard adipogenic differentiation protocol for 9 days before cells were serum starved for 1 hour. Cells were treated with 1 μM 12,13-diHOME or methyl acetate vehicle in 0.1% w/v BSA in PBS for 15 minutes before the culture medium was removed, and cells were incubated with DMEM/H containing 4% FA-free BSA w/v in PBS, 0.5 mM palmitic acid, and 0.2 μCi/mL [1-^{14}C]-palmitic acid (PerkinElmer Life and Analytical Science, Waltham, MA) for 1 h. The incubation medium was transferred to a vial containing 1M acetic acid, capped quickly, and allowed to incubate for 1 h for CO_2 gas to be released. [14] The CO_2 released was absorbed by hyamine hydroxide, and activity was counted. FA oxidation was calculated from CO_2 generated. To measure fatty acid uptake, cells were rinsed twice with PBS and lysed after incubation with [1-^{14}C]-palmitic acid. Lipids were extracted using a chloroform-methanol mixture (2:1), and ^{14}C-counts were determined in the organic phase. Protein concentrations were determined by using the Pierce BCA kit (Life Technologies) according to instructions, and FA uptake (^{14}C lipids in the cells) and oxidation ($^{14}CO_2$ generated) were normalized to protein content. All cells were confirmed to be Mycoplasma free.

Seahorse Bioanalyzer

WT-1 brown preadipocytes were seeded onto gelatin coated Seahorse Plates and differentiated according to standard protocols. Cells were starved for 1 h, then treated for 15 min with 1 μM 12,13-diHOME or methyl acetate vehicle. The oxygen consumption rates (OCR) were monitored in 200 μM palmitic acid plus 100 μM albumin in a Seahorse XF24 instrument using the standard protocol of 3 min mix, 2 min wait, and 3 min measure. For the normalization of respiration to protein content, cells were lysed in RIPA buffer and protein concentration was measured using the Pierce BCA kit (Life Technologies).

Membrane Fractionation

WT-1 brown preadipocytes were differentiated according to a standard adipogenic differentiation protocol for 9 days before cells were serum starved for 1 hour. Cells were treated with 1 μM 12,13-diHOME or methyl acetate vehicle in 0.1% BSA w/v in PBS for 15 minutes before cells were scraped from tissue culture plates into homogenization buffer and membranes were separated according to previously published protocols[37]. Protein lysates were stored at -20°C until further use. Protein concentrations were determined by using the Pierce BCA kit (Life Technologies) according to instructions. For immunoblots, lysates were diluted into Laemmli buffer and boiled, then loaded onto 10 % Tris gels for SDS-PAGE. After complete separation of the proteins, these were transferred on a PVDF membrane (Amersham Biosciences), blocked in western blocking buffer (Roche) and primary antibodies (Antibody Table) were applied in blocking buffer over night at 4 °C. After washing 4 x for 15 min with TBS-T, secondary antibodies were applied for 1 h in blocking buffer. Membranes were washed again 3 x times for 15 min in TBS-T and developed using chemiluminescence (ThermoFisher). After scanning films, densitometry was analyzed using ImageJ software. All antibodies are listed in Supplementary Table 4.

Statistics

No statistical method was used to predetermine sample size. All experiments were not blinded. All statistics were calculated using Microsoft Excel, Graphpad Prism and RStudio using LIMMA package. In all cases, we assumed equal variance. For consistency, the Spearman correlation coefficient is shown however all Pearson and Kendall coefficients reached similar levels of significance. For all correlation coefficients, p value was calculated using algorithm AS 89[38].

SUPPLEMENTARY REFERENCES (METHODS)

34. Tseng, Y.H., Kriauciunas, K.M., Kokkotou, E. & Kahn, C.R. Differential roles of insulin receptor substrates in brown adipocyte differentiation. *Mol. Cell Biol* **24**, 1918-1929 (2004).
35. Kloting, N.*, et al.* Insulin-sensitive obesity. *Am J Physiol Endocrinol Metab* **299**, E506-515 (2010).
36. Powell, W.S. Extraction of eicosanoids from biological fluids, cells, and tissues. *Methods Mol Biol* **120**, 11-24 (1999).
37. Nishiumi, S. & Ashida, H. Rapid preparation of a plasma membrane fraction from adipocytes and muscle cells: application to detection of translocated glucose transporter 4 on the plasma membrane. *Bioscience, biotechnology, and biochemistry* **71**, 2343-2346 (2007).

38. Best, D.J. & Roberts, D.E. Probabilities of Spearman's rho. *Applied Statistics* **24**, 377-379 (1975).

Supplementary Figure 1

Annotation of lipid species profiled by LC-/MS in human and mouse serum and mouse adipose tissues. (a) Dendrogram of all lipids included in the initial screen according to their original fatty acid and enzymatic pathway. (b) For all lipid species measured by LC-MS/MS annotation of, whether the lipid was pro- or anti-inflammatory.

Supplementary Figure 2

Lipid species changed by a one-hour cold challenge. The increase in abundance of three lipid species reached a nominal p value of 0.05 after cold exposure. The two species with lower significance were only detectable after cold exposure.

Supplementary Figure 3

Anthropometric correlates of 12,13-diHOME. (a-i) Circulating 12,13-diHOME concentration plotted against age (a), fasting plasma insulin (FPI) (b), fasting plasma glucose (FPG) (c), hemoglobin A1c (HbA1c) (d), C-reactive protein (CrP) (e), circulating leptin (f), circulating total cholesterol (g), circulating aspartate transaminase (ASAT) (h), and circulating gamma-glutamyl transpeptidase (gGT) (i). In each panel, R is the Spearman correlation coefficient and males are shown in blue while females are shown in pink. N=55 individual subjects (13 M/42 F). (j) Circulating 12,13-diHOME in each body mass index (BMI) category. Data are presented as normalized means ± s.e.m.; n=15 lean, 13 overweight and 27 obese subjects. (k) Circulating 12,13-diHOME in each BMI category of males and females. Data are presented as normalized means ± s.e.m.; n=15 lean (4 M/11 F), 13 overweight (4 M/9 F) and 27 obese subjects (5 M/22 F); *$p<0.05$ by t-test. (l) Circulating 12,13-diHOME in each BMI category of subjects with normal glucose tolerance (NGT) or Type 2 diabetes (T2D). Data are presented as normalized means ± s.e.m.; n=15 lean, 13 overweight (10 NGT/3 T2D) and 27 obese subjects (20 NGT/7 T2D).

Supplementary Figure 4

12,13-biosynthesis in cold activated adipose tissue. (a) 12,13-diHOME concentrations measured by LC-MS/MS in serum from wild type and *Myf5*^{cre}*BMPr1a*$^{f/f}$ mice housed at cold or thermoneutral for 2 or 11 days. Data are plotted as the normalized means ± s.e.m.; n=5 WT thermoneutral males, 5 WT cold males, 4 *Myf5*^{cre}*BMPr1a*$^{f/f}$ thermoneutral males, 5 *Myf5*^{cre}*BMPr1a*$^{f/f}$ cold males, 3 WT thermoneutral females, 2 WT cold females,

4 *Myf5*^{cre}*BMPr1a*$^{f/f}$ thermoneutral females, 1 *Myf5*^{cre}*BMPr1a*$^{f/f}$ cold female; *p<0.05 by t-test. (b) *Ephx* family gene expression measured by qPCR in different tissues from mice housed at cold or thermoneutrality for 7 days. Data are plotted as the means normalized to thermoneutrality ± s.e.m.; n=8 per group; *p<0.05 by t-test. (c) Meta-analysis of 4 publically available BAT gene expression datasets from mice exposed to cold for different lengths of time for genes in the 12,13-diHOME biosynthetic pathway. The induction by cold of each gene after cold exposure is shown by increased fold change on the y axis. (d) 12,13-diHOME concentrations measured in different mouse tissues. Data are means +/- s.e.m.; n= 8 mice; *p<0.05, **p<0.005 , ***p<0.0005 by t-test. (e) 12,13-diHOME concentrations measured by LC-MS/MS in sWAT from wild type and *Myf5*^{cre}*BMPr1a*$^{f/f}$ mice housed at cold or thermoneutral for 2 or 11 days. Data are plotted as the normalized means ± s.e.m.; n=5 WT thermoneutral males, 5 WT cold males, 4 *Myf5*^{cre}*BMPr1a*$^{f/f}$ thermoneutral males, 5 *Myf5*^{cre}*BMPr1a*$^{f/f}$ cold males, 3 WT thermoneutral females, 2 WT cold females, 4 *Myf5*^{cre}*BMPr1a*$^{f/f}$ thermoneutral females, 1 *Myf5*^{cre}*BMPr1a*$^{f/f}$ cold female; *p<0.05 by t-test. (f) *Ephx1* gene expression measured by qPCR in BAT and sWAT from mice treated daily with 1 mg/kg body weight CL316,243 intraperitoneally for 10 days. Data are presented as normalized means ± s.e.m.; n=6 per group; *p<0.05 by t-test. (g) *Ephx2* gene expression measured by qPCR in BAT and sWAT from mice treated daily with 1 mg/kg body weight CL 316,243 intraperitoneally for 10 days. Data are presented as normalized means ± s.e.m.; n=6 per group; *p<0.05 by t-test.

Supplementary Figure 5

Physiologic effects of acute 12,13-diHOME treatment in mice. (a) Pulse measured in the tail after pretreatment with 12,13-diHOME or vehicle. Data are means ± s.e.m.; n=6 per group. (b) Systolic pressure measured in the tail vein after pretreatment with 12,13-diHOME or vehicle. Data are means ± s.e.m.; n=6 per group. (c) Diastolic pressure measured in the tail after pretreatment with 12,13-diHOME or vehicle. Data are means ± s.e.m.; n=6 per group.

Supplementary Figure 6

Physiologic effects of daily 12,13-diHOME injections. (a) Body weights over 7 day course of daily injection treatment. Data are means +/- s.e.m.; n=6 treated vs. 5 controls. (b) Glucose tolerance test of a separate cohort of diet-induced obesity mice treated every other day for 2 weeks with either 12,13-diHOME or vehicle. Data are means +/-

s.e.m.; n=5 per group. (c) Serum non-esterified free fatty acids (FFA) of mice treated daily for one week with either 12,13-diHOME or vehicle. Data are means +/- s.e.m.; n=6 treated vs. 5 controls. (d) mRNA expression measured by qPCR of UCP1 and *LPL* in tissue from mice treated every other day for two weeks with either 12,13-diHOME or vehicle. Data are means +/- s.e.m.; n=6 treated per group; *p<0.05 by t-test. (e) Oral lipid tolerance test showing serum triglyceride concentration from mice treated with vehicle or 12,13-diHOME and then given an oral bolus of triglyceride. Data are means ± s.e.m.; n=6 per group; *p<0.05 by ANOVA with post-hoc Bonferroni test. (f) Radioactivity per 10 mg of tissues from mice treated with vehicle, Norepinephrine (NE) or 12,13-diHOME and then given a bolus of radiolabeled glucose. Tissues were measured by scintillation counting in liver, gastrocnemius muscle (Gastroc), soleus muscle, heart, BAT, sWAT, and epididymal white adipose tissue (eWAT). Data are means ± s.e.m.; n=8 per group; *p<0.05 12,13-diHOME vs. Vehicle by ANOVA with post-hoc Bonferroni test.

Supplementary Figure 6
Un-cropped immunoblots shown in this manuscript.

Supplementary Table 1
Lipid profiling by LC-MS/MS in human plasma after saline or cold challenge.

Supplementary Table 2
P values for linear model of relationship between each phenotype with BMI as covariate.

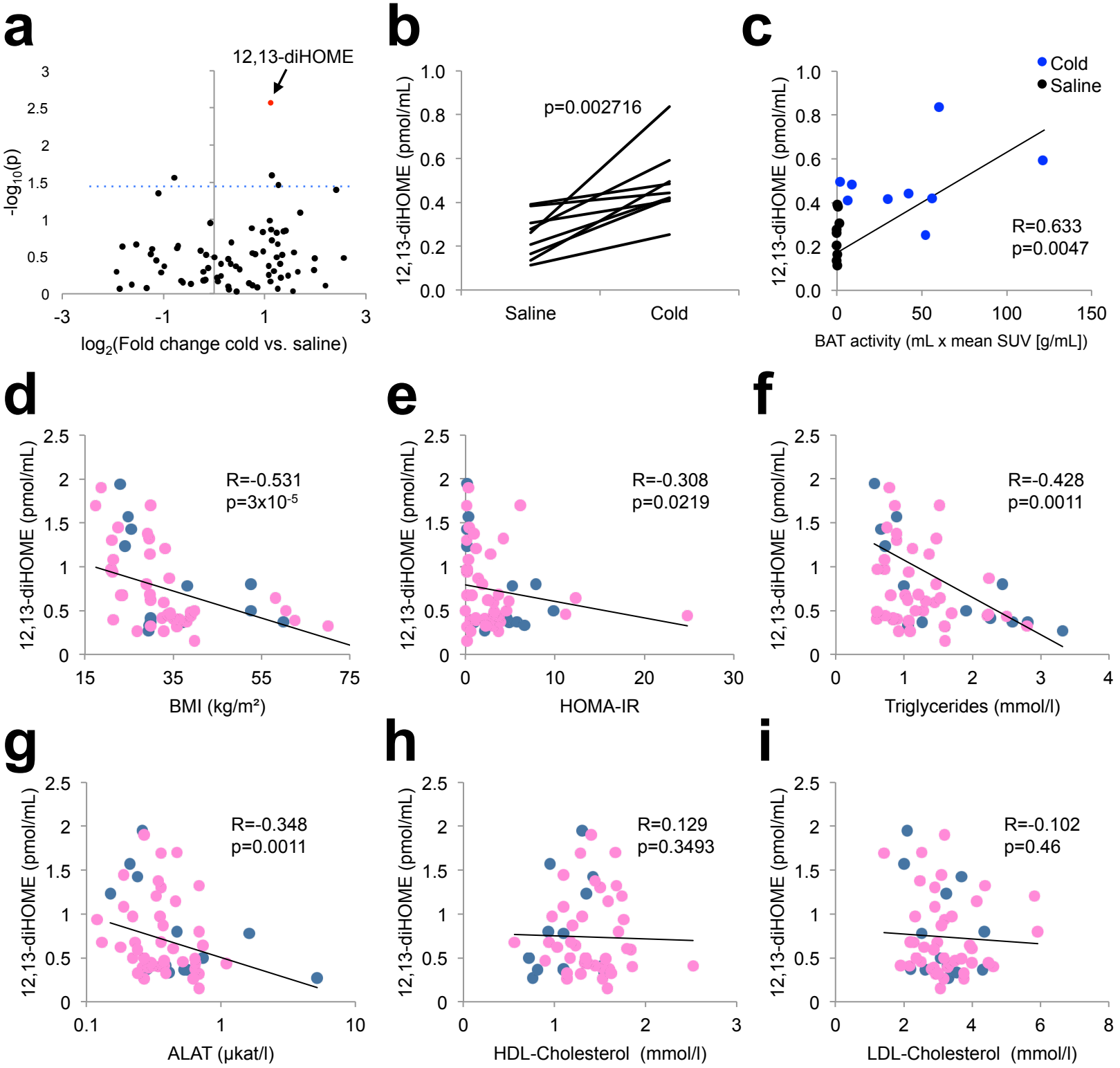
Supplementary Table 3
Primer Sequences.

Supplementary Table 4
Antibodies.

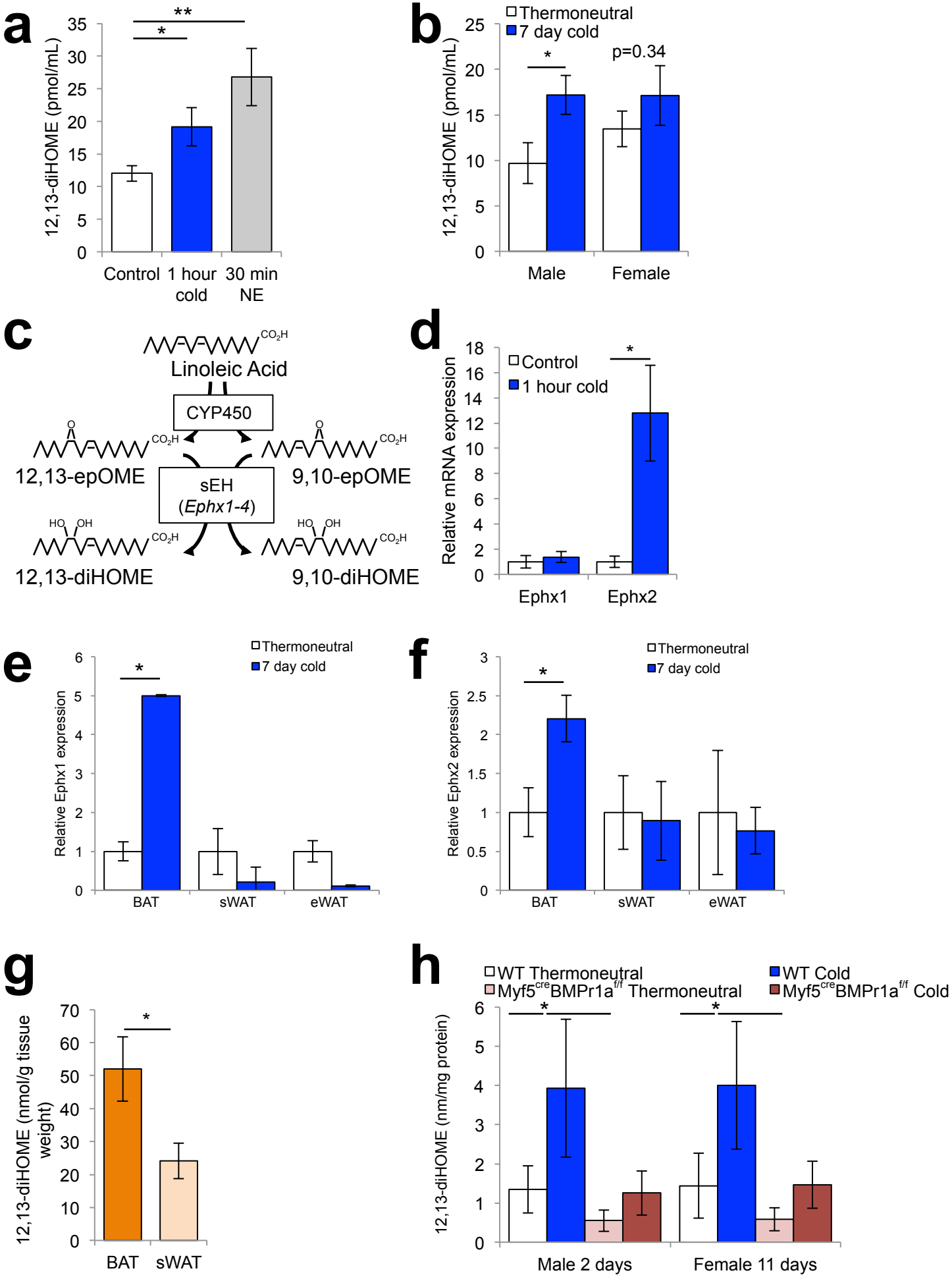
Supplementary Video 1
Representative imaging of FFA-SS-Luc uptake in UCP1cre$^{+/-}$Rosa(stop)Luc$^{+/-}$ injected intravenously with luciferin-conjugated fatty acid and 12,13-diHOME or vehicle. Data from individual images using sequential one-minute exposures over approximately 50 minutes was stacked into a movie. The animal on the left is the vehicle treated and the mouse on the right is treated with 12,13-diHOME.

Supplementary Video 2

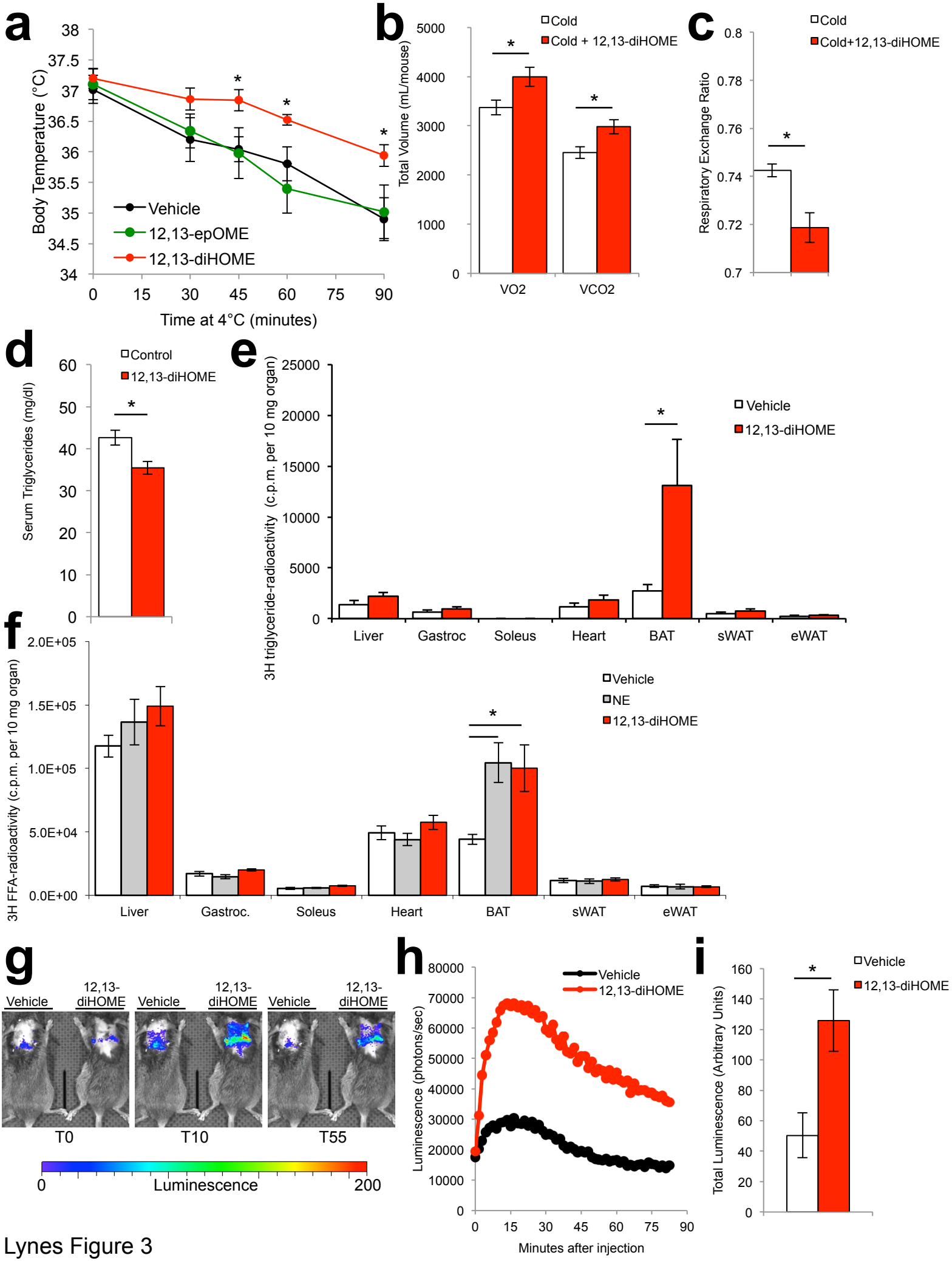
Representative imaging of FFA-SS-Luc uptake in CAG-Luc$^{+/+}$ brown adipocyte cells treated with 12,13-diHOME or vehicle and then incubate with luciferin-conjugated fatty acid. Data from individual images using sequential 30 second exposures over approximately 50 minutes was stacked into a movie. The well on the left is vehicle treated and the well on the right is treated with 12,13-diHOME.



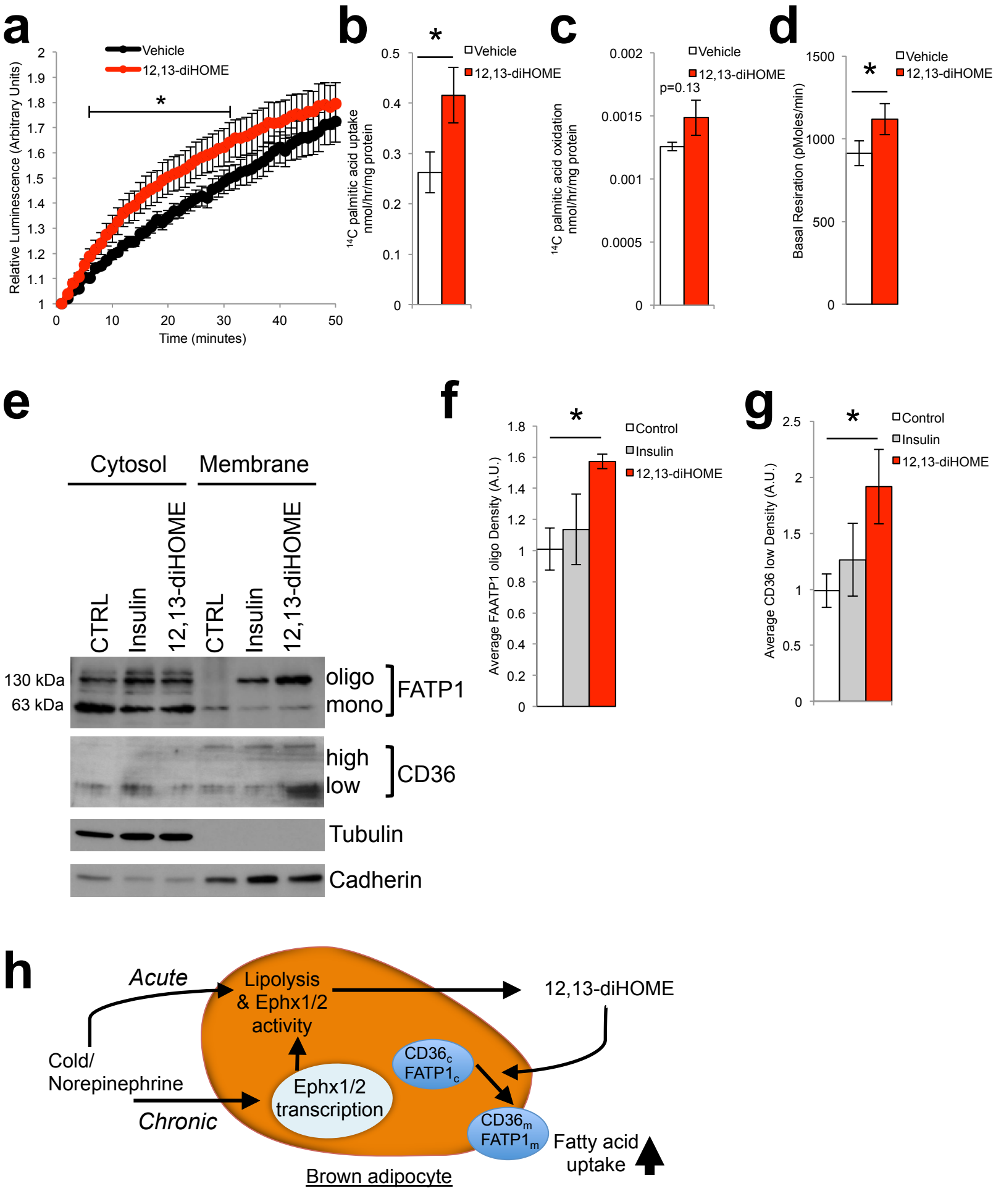
Lynes Figure 1



Lynes Figure 2

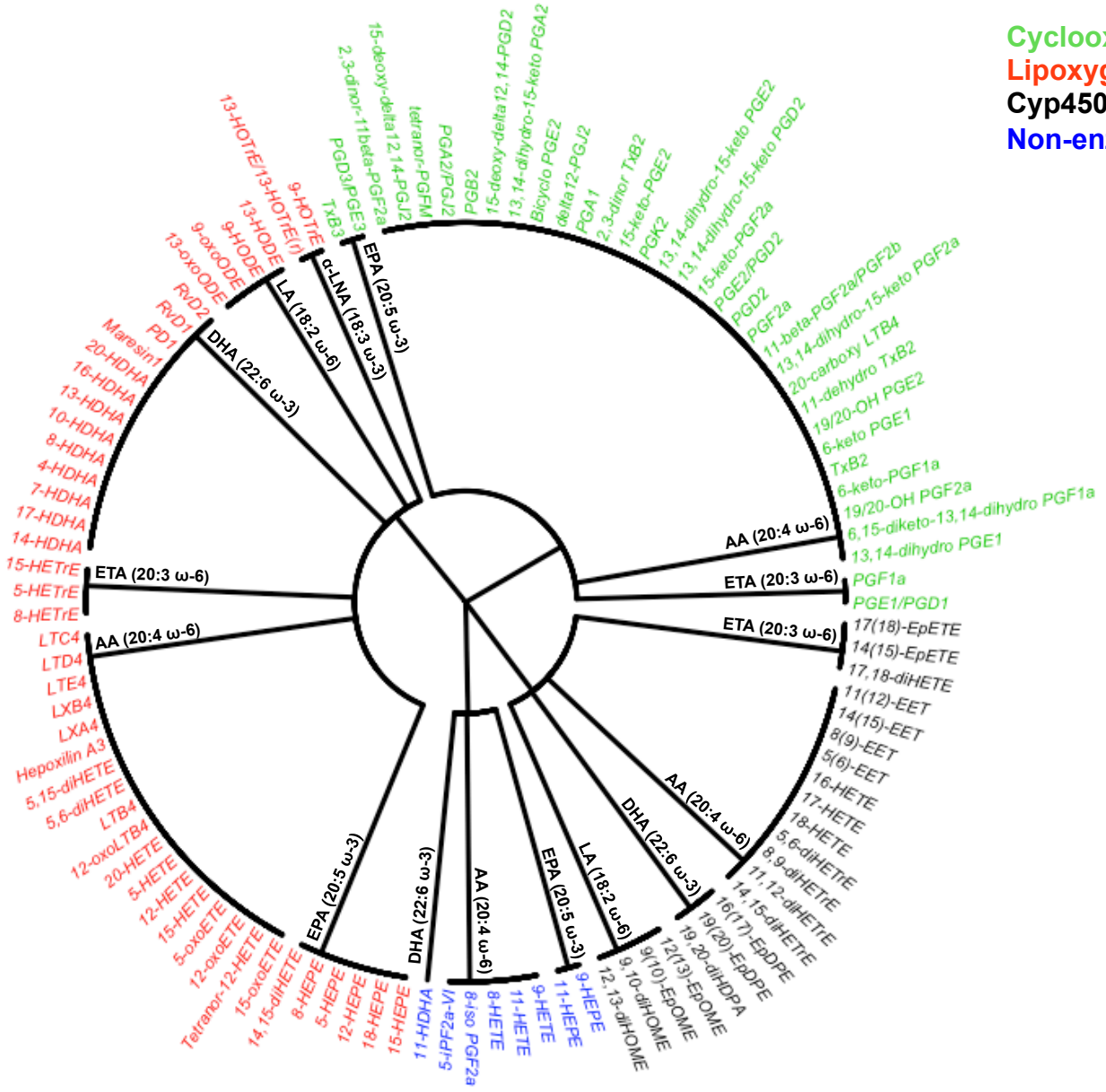


Lynes Figure 3

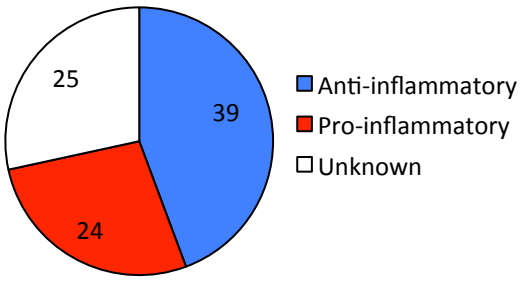


Lynes Figure 4

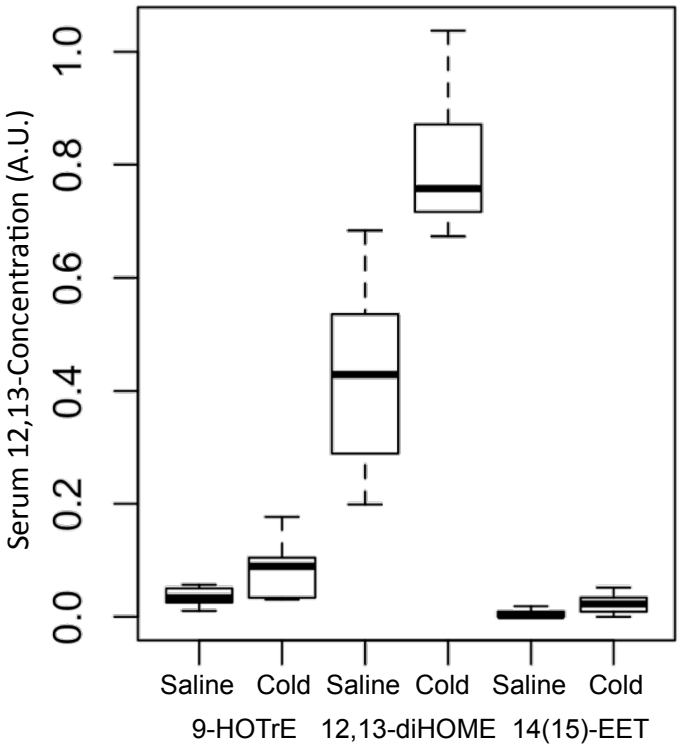
a



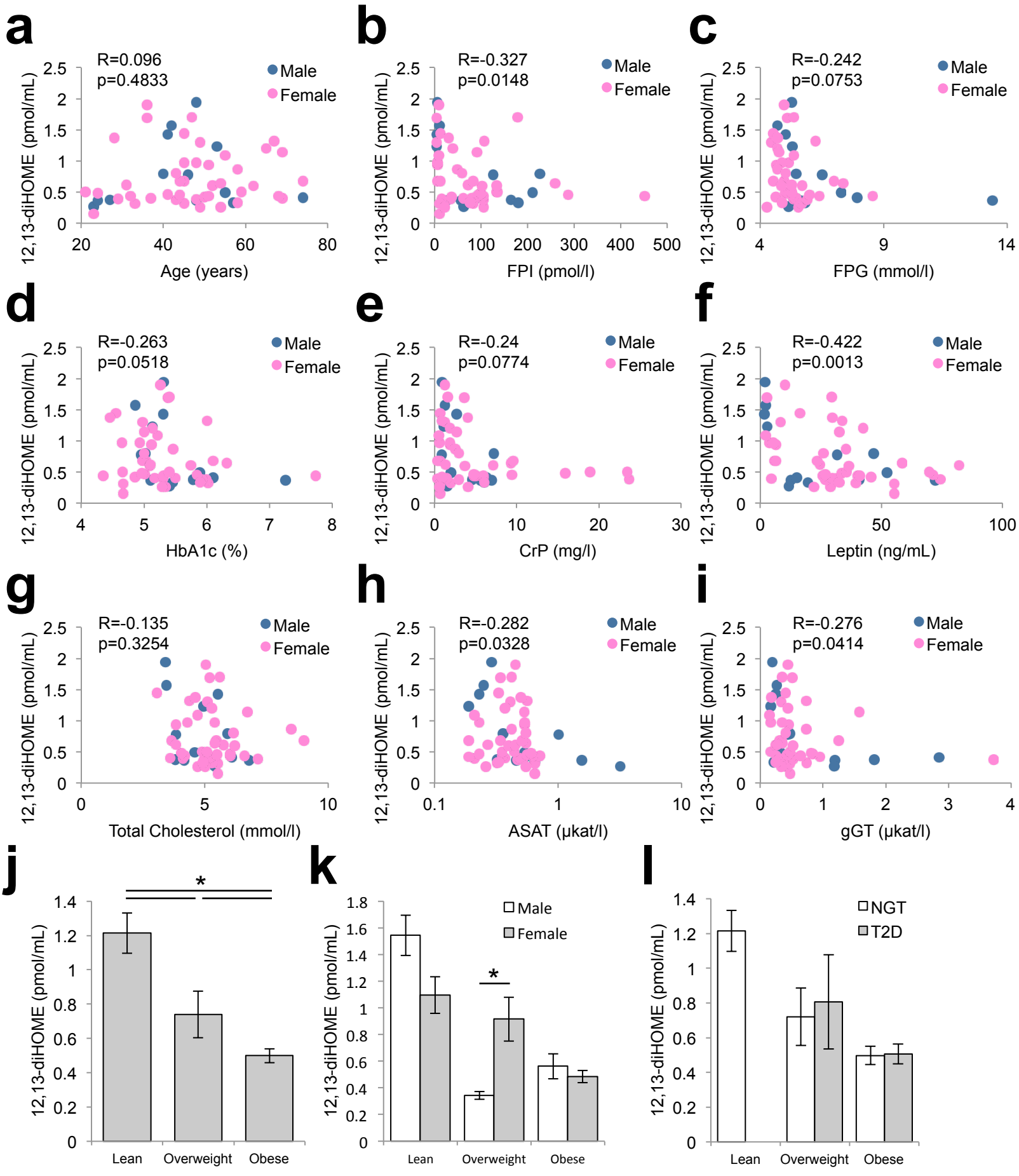
b Inflammatory effect



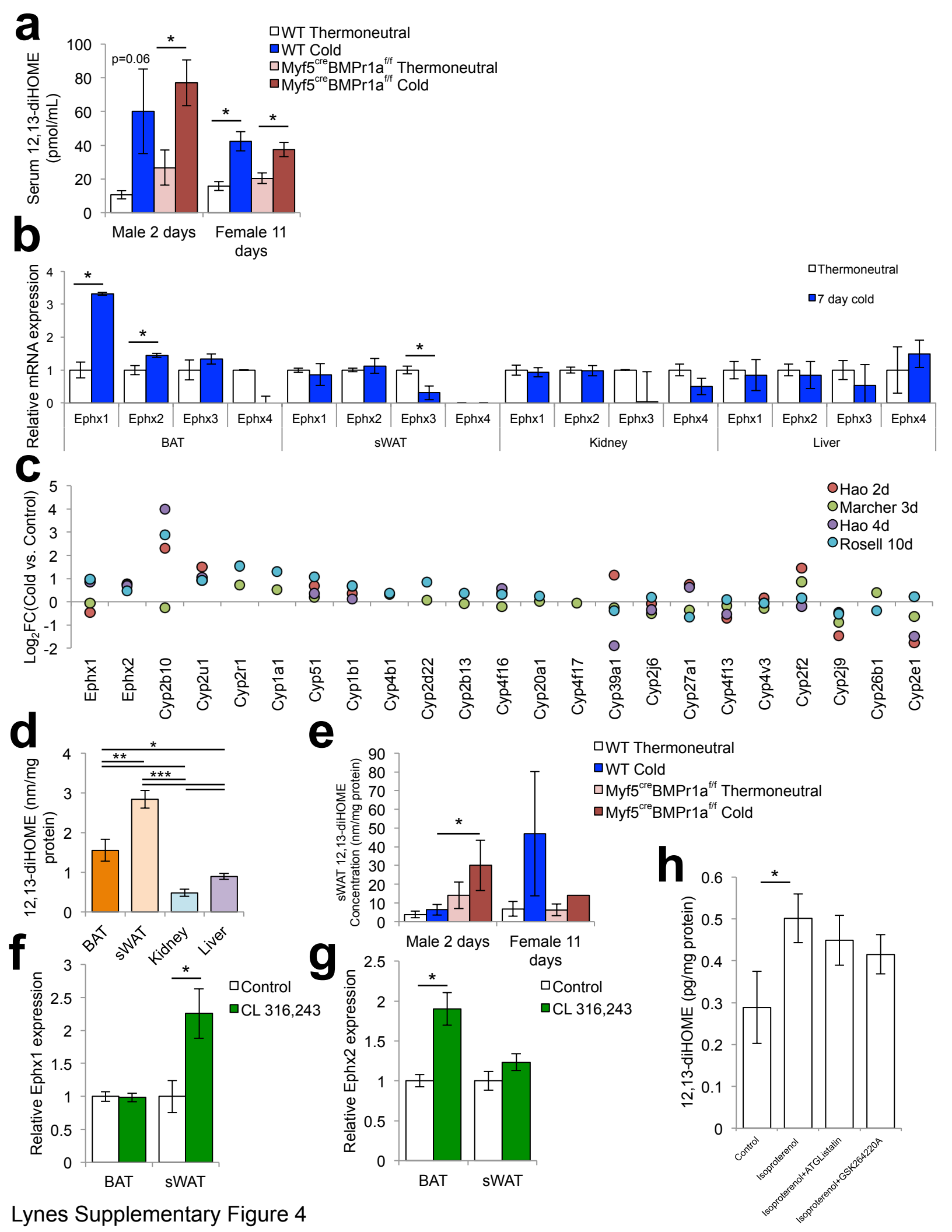
Lynes Supplementary Figure 1



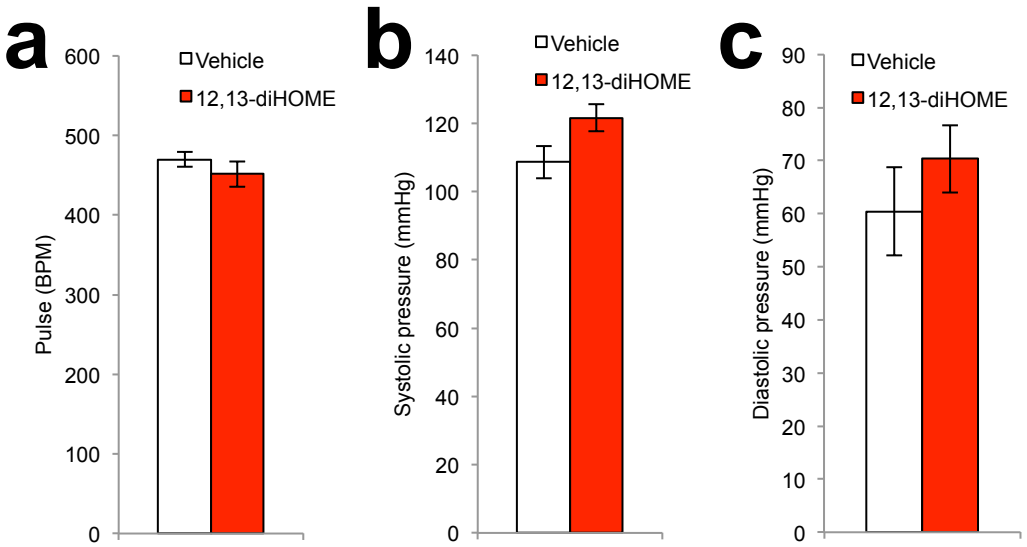
Lynes Supplementary Figure 2



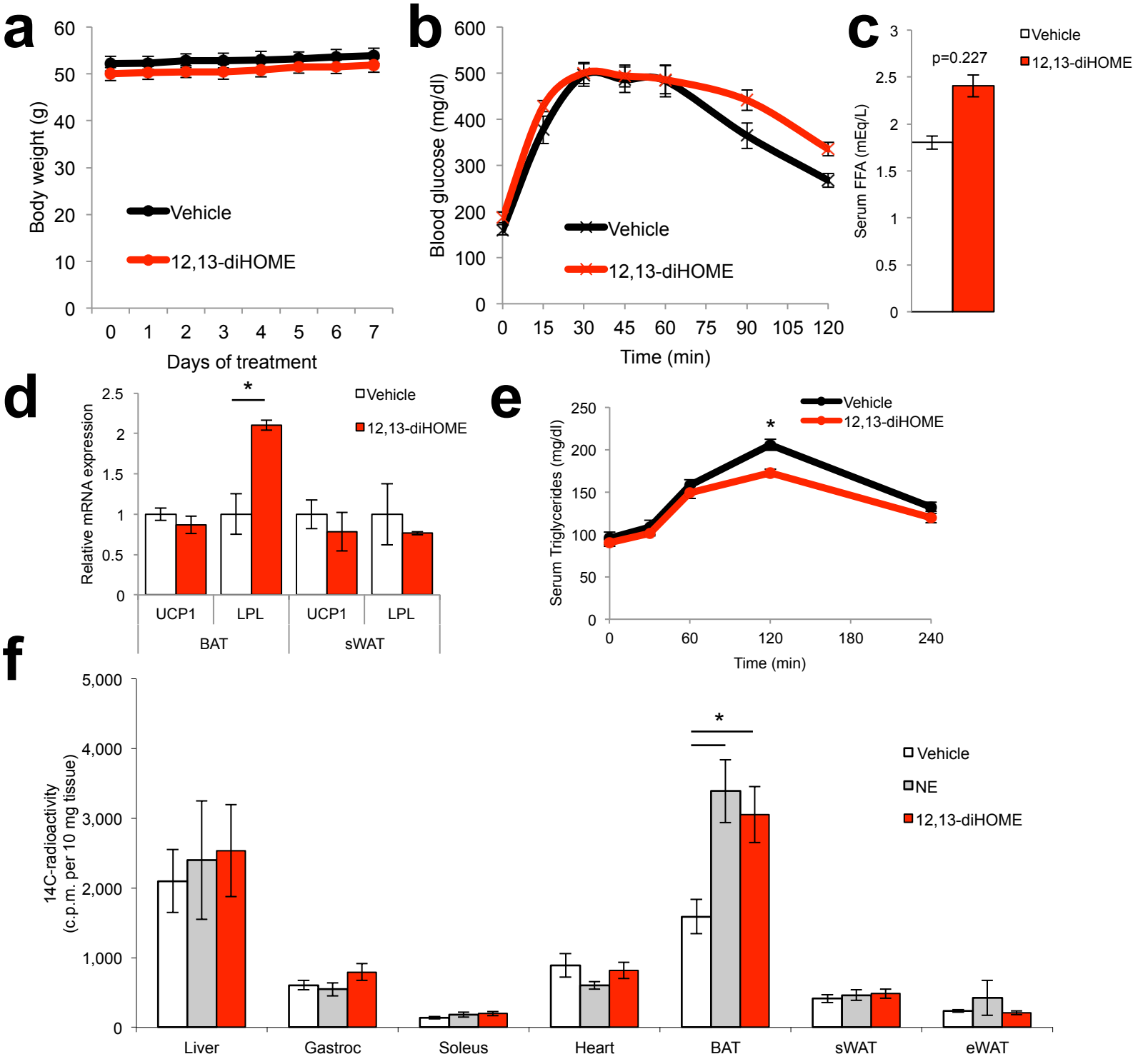
Lynes Supplementary Figure 3



Lynes Supplementary Figure 4



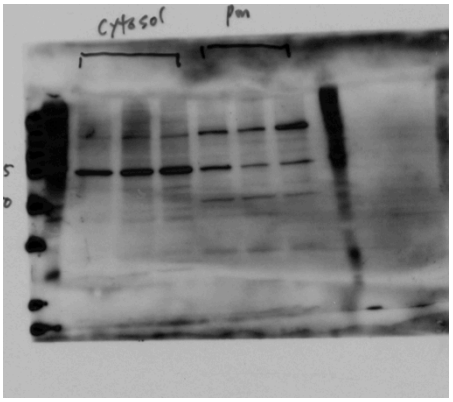
Lynes Supplementary Figure 5



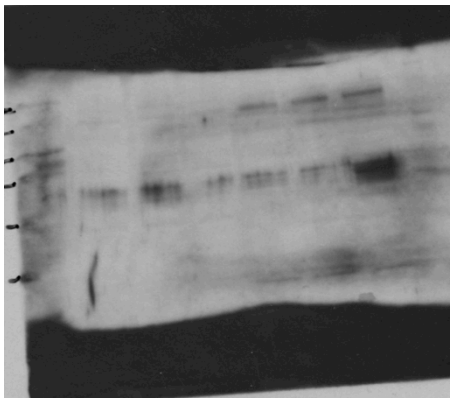
Lynes Supplementary Figure 6

Cytosol Membrane

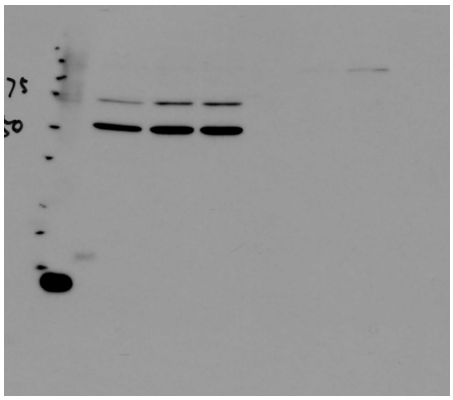
Control
Insulin
12,13-diHOME
Control
Insulin
12,13-diHOME



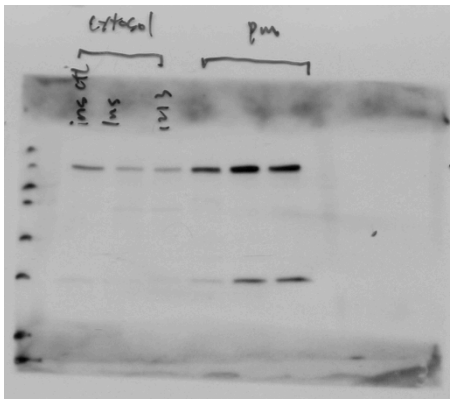
FATP1



CD36



Tubulin



Cadherin

Lynes Supplementary Figure 7

Subject	341-01	341-02	341-03	341-04	341-05	341-06	341-07	341-08	341-09	341-01	341-02	341-03	341-04	341-05	341-06	341-07	341-08	341-09
Treatment	Cold	Cold	Cold	Cold	Cold	Cold	Cold	Cold	Cold	Saline	Saline	Saline	Saline	Saline	Saline	Saline	Saline	Saline
Code	341-01-C	341-02-C	341-03-C	341-04-C	341-05-C	341-06-C	341-07-C	341-08-C	341-09-C	341-01-S	341-02-S	341-03-S	341-04-S	341-05-S	341-06-S	341-07-S	341-08-S	341-09-S
Species																		
IS-d4-9-HODE	0	0	0	0	0	0	0	0	0	0	0	0	0	0	0	0	0	0
9-oxoODE	0.8820752	0.13772466	0.30110357	0.40821832	0.46119151	0.38578526	0.53432263	0.11439154	1.66230684	0.22070346	0.13464997	0.67824337	0.33963432	0.12871609	0.16220992	0.06446726	0.36655777	0.6221771
13-oxoODE	0.84687575	0.23180595	0.08310963	0.37735672	0.44132719	0.37386546	0.38222553	0.13517607	1.23434785	0.14931878	0.16398264	0.44110481	0.29814292	0.11087036	0.14897919	0.03521053	0.18031766	0.47868483
9-HOTrE	0.17697993	0.03389002	0.09420009	0.10592884	0.0370685	0.03113476	0.10456824	0.03061817	0.09664619	0.05040424	0.03213139	0.03560318	0.05618638	0.0291903	0.01039693	0.02553466	0.04993029	0.05675979
13-HOTrE/13-HOTrE(r)	0	0.00212058	0.08444003	0.05244116	0.03325706	0.02123659	0.08367766	0.08187226	0.01455282	0.07389398	0.03267962	0.31266571	0.09382568	0.00671887	0.01854387	0.0355627	0.04223872	0.12527225
9-HODE	3.91943541	1.22345046	0.67334838	1.31061089	1.86791051	1.0102823	1.96652953	0.94789946	5.64421903	1.59699636	0.42535328	3.18619718	1.30629673	0.52118429	0.54076628	0.56493647	0.95049219	4.60993797
13-HODE	5.12097498	1.12833588	0.82558584	1.75618796	2.63683682	1.34057854	2.45533991	1.16158199	8.28243273	1.62602974	0.47028437	3.37096622	2.23948275	0.54787381	0.62625744	0.67280668	1.20385351	2.7311558
9(10)-EpOME	2.20215408	0.74125195	0.31476495	0.27484368	0.53126437	0.37912148	0.71423327	0.49946771	1.97850056	0.40949975	0.28451051	1.80132934	0.83020776	0.21822925	0.12019162	0.05716339	0.50686715	0.24733913
12(13)-EpOME	1.87320275	0.79379427	0.41317053	0.4362924	0.57413432	0.47966661	0.80479263	0.54021352	2.49837296	0.4873635	0.46113654	1.67584874	0.91390139	0.25161919	0.24222062	0.0865	0.60470406	1.58567437
9,10-diHOME	3.3272534	0.90768129	0.99019041	0.57254189	0.87079847	0.56103895	0.98862293	1.19871882	1.18568809	0.49795281	1.162309	0.52972917	0.8081577	0.41988789	0.24595267	0.35718634	1.2049586	0.77173535
12,13-diHOME	1.46875726	0.71652283	0.73638901	0.77912647	0.7267959	0.44177781	0.87098188	1.03721686	0.84714557	0.4575017	0.53594509	0.36370236	0.67222662	0.28907866	0.19869644	0.23709389	0.48616595	0.6838185
18-HEPE	0.03482791	0.0226062	0.01393433	0.00128854	0.00452034	0.04189755	0.01187777	0	0.01691096	0	0.01633175	0.03412209	0.04322722	0.00749832	0	0	0	0.00599058
15-HEPE	0.03995867	0	0.02781801	0.00839931	0.00649814	0.01278576	0.02861311	0.03783117	0.01252254	0.00648206	0.07548249	0.00512205	0.0336037	0.00278939	0.0487373	0.03779358	0.01255589	0.01465769
12-HEPE	0.03797506	0	0.00669321	0.00331692	0	0	0.00649222	0	0.0059629	0.01480579	0	0	0.02927001	0	0.01122213	0.03477062	0	0.00410264
5-HEPE	0.01443379	0.0089581	0.00591013	0.00831136	0	0.03951262	0.03103896	0	0	0.02850702	0.02693501	0.01779496	0.00432579	0	0.00423175	0.02931917	0.00846928	0.00333205
11-HEPE	0.02045306	0	0	0.00310293	0	0.01149639	0.00475933	0	0.0039127	0	0.01437334	0	0.01895096	0	0	0	0.01279124	0.00417701
8-HEPE	0.01577257	0.02781498	0	0	0.00814537	0.02094913	0	0.01078564	0	0	0	0	0.0086514	0	0.00862009	0.02288272	0.0084697	0
15-oxoETE	0.01796359	0.00426954	0	0.00675241	0	0.0153798	0.00570874	0.03426826	0	0	0.04323442	0	0	0.00548504	0.00458438	0	0	0.0038982
9-HEPE	0	0	0	0	0	0	0	0	0.00426522	0	0	0	0	0.00354795	0	0	0	0
14(15)-EET	0.02118569	0.05183913	0	0.00918021	0	0.00997707	0.024636	0.03407762	0.04587191	0.00648871	0	0	0.00432557	0	0.01722086	0	0.00919167	0
11(12)-EET	0.01578896	0.034617	0.04466404	0	0.02181022	0	0.00640353	0.05752618	0.05576792	0.01881642	0.04062346	0.00531622	0.00168112	0.00278909	0.02441701	0.02822197	0	0.00961029
8(9)-EET	0	0.05018695	0.00929148	0.01584103	0	0.04858976	0.02459868	0.00464922	0	0.0345319	0.10462385	0.02023739	0	0.00957971	0.03720013	0.00530879	0.01693959	0.00449927
5(6)-EET	0.00643152	0.00161645	0	0	0.00800458	0.01278646	0.03103985	0.03556599	0.0229632	0.01482362	0.05393147	0.01920405	0.00432579	0.00154816	0	0	0.03802619	0.00381695
15-HETE	0.07191695	0.04967329	0.05489717	0.02421615	0.0182332	0.03551278	0.06858253	0.13475127	0.04767125	0.08072385	0.11617988	0.01358925	0.04751897	0.02529085	0.02811637	0.03147345	0.01461535	0.03664841
12-HETE	0.1665798	0.08207757	0.04170098	0.03502899	0.04040702	0.14849331	0.27205378	0.11740046	0.04314802	0.04076668	0.24696941	0.02658043	0.08995519	0.02911897	0.0248371	0.92245723	0.00872025	0.05640258
5-HETE	0.14201379	0.15667264	0.11004592	0.0491466	0.02794356	0.20771158	0.24605791	0.23871839	0.20932031	0.19722658	0.31201862	0.08347809	0.04301536	0.02577249	0.05942672	0.08752551	0.12765647	0.09497188
20-HETE	0.05374696	0.13715509	0.02223985	0.01021937	0.00608212	0.01917904	0.01598946	0.00464922	0.08172544	0.06587482	0.07824381	0	0	0.00294681	0.02229653	0.00535926	0.00768525	0.01374217
11-HETE	0.15478346	0.11454226	0.01821948	0.04501689	0.02968725	0.10309355	0.06475798	0.18665149	0.15898088	0.11062228	0.09429788	0.01316201	0.29821177	0.07710361	0.07707103	0.70649298	0.08582017	0.04986108
16-HETE	0.04581254	0.00849749	0.03481581	0.01900474	0	0.02185598	0.01627169	0.01175279	0.0177593	0.01206397	0.02780117	0.00960223	0.00397036	0	0.03448142	0	0.01086333	0.00711744
17-HETE	0	0.11589514	0.0831147	0.01190338	0.02470268	0.0416021	0	0.07104636	0	0.04626907	0.20026577	0.06238974	0.12378804	0.02452737	0.04716968	0.01727634	0.24170241	0.02718897
18-HETE	0.02976464	0.03681365	0.00921048	0.01917963	0	0.07672836	0	0.10356622	0.07710787	0.07537659	0.19277452	0.03436163	0.03017551	0.04201908	0.05321102	0	0	0.01730326
9-HETE	0.00643083	0.04239607	0	0	0	0.0055111	0	0	0.00913759	0.03682737	0.02874102	0.00531599	0.00432558	0.00393721	0	0.03985586	0	0.01199032
8-HETE	0.0336904	0.04170806	0	0.01531632	0.00899042	0.00850767	0.00991709	0.03182722	0.00539254	0	0.05428681	0.01801625	0.07517357	0	0	0.06338788	0.03307261	0.01220137
all trans-LTB4	0.01327579	0.03598697	0	0	0.00501076	0.00775905	0	0.00218906	0.02369955	0.01036466	0	0	0.0087393	0.00843015	0	0	0.0038656	0
LTB4	0.01327579	0.00520328	0	0	0.00501076	0.00775905	0	0.01285761	0	0	0	0.00249753	0.00708181	0	0	0	0	0
5,6-diHETE	0.04434704	0.01750288	0.0114727	0.00961816	0	0.01576784	0	0	0.00801009	0.01258684	0	0.00082286	0	0	0.00878691	0.00395142	0	0.00109043
5,15-diHETE	0	0	0	0	0	0	0	0	0.0049252	0	0.00752271	0	0	0	0.00570484	0	0	0
Hepoxilin A3	0.01265234	0	0.01071905	0	0	0	0	0	0	0	0.01362103	0	0	0	0	0.00452613	0.00386563	0.00766148
17-HDHA	0.13086115	0.03094994	0	0	0	0	0.0633934	0.14383265	0	0	0	0.02119478	0	0.08715058	0	0	0.01418545	0.008345
14-HDHA	0.01104692	0.03963729	0.00923092	0.00331692	0.00223335	0.02095718	0.00401189	0.04854841	0.00596288	0.03129745	0.03253428	0	0	0.00787485	0	0.1217398	0	0.00435603
7-HDHA	0	0.00520821	0	0.00371737	0	0.03399313	0.02354642	0	0	0	0	0.00512305	0.00432564	0	0	0	0	0.00435581
4-HDHA	0.0222041	0	0.00925261	0.00780255	0.00606823	0.02094808	0.02561428	0	0.01192581	0	0.02693615	0	0.0231951	0.00546205	0.02171119	0.02822318	0.01547035	0.00416748
8-HDHA	0.01626243	0	0	0	0	0.02094824	0.03876309	0	0.02739624	0	0	0.00450554	0.01895612	0	0	0	0	0.00416525
10-HDHA	0.0157719	0.02205848	0.03543268	0	0.00904059	0	0	0.03117691	0	0	0.01484626	0.01491797	0.00432579	0.00812764	0.01425676	0.00531269	0	0
11-HDHA	0	0	0.01846295	0	0	0	0	0.00881858	0	0	0.05170875	0	0	0.00278911	0	0.02888005	0	0.00434652
13-HDHA	0.02699201	0	0.00923194	0.00331681	0.00608207	0	0.01280712	0.04021322	0.00596318	0	0.04690383	0	0.06286332	0.00920093	0	0.0884625	0.0311973	0
16-HDHA	0	0.01402686	0.00923179	0.00521808	0.00452035	0.00787255	0.00946175	0.03556135	0	0	0.05051611	0.00669153	0.00222847	0.00932429	0.00860048	0.07601718	0.00846921	0.00600437
20-HDHA	0	0.00519654	0.03543118	0.01199923	0	0.03154359	0.00476209	0.01793754	0.0229103	0.06892118	0.05129034	0.00888749	0	0.01044571	0	0.0244436	0.01040728	0.01345364
19(20)-EpDPE	0	0.00519654	0.00477116	0	0	0	0	0.01286167	0	0.06750689	0	0	0	0.00934214	0	0.02291146	0	0
16(17)-EpDPE	0	0.00169609	0	0	0	0	0	0.04020443	0	0.01480579	0	0.02451986	0.00419905	0.00492333	0	0.02291011	0.01471839	0
PGE2/PGD2	0.03237649	0.03311641	0.00162726	0	0.00263481	0.0154526	0	0.01966326	0.00613352	0.00180509	0.00403581	0.00601951	0.00436398	0.02118443	0.00148337	0.04024763	0.00934356	0.00283751
PGD2	0.05110797	0	0.00299722	0.00310629	0	0.00786371	0.00534238	0.00539098	0.00955062	0	0.00382797	0.0020889	0.00276077	0	0.00328019	0.0218241	0	0.0032589
LXA4	0.03969985	0.01253619	0.00335969	0	0	0	0	0	0.0033298	0.00564954	0	0.00862614	0.00766044	0.00323691	0	0	0	0.00104566
LXB4	0.00214888	0.00283358	0.00318569	0.0060449	0.00517021	0.00518695	0.01116179	0	0.00194575	0.01881837	0.02066103	0	0	0.02335869	0	0.01220011	0	0.001208
15-keto-PGF2a	0	0	0.00368083	0	0	0.00353299	0.01212309	0	0.01668138	0.018012	0.0028776	0.00166392	0	0.00866126	0.00045731	0.00204585	0.0031371	0.00216842
13,14-dihydro-15-keto PGE2	0.00476807	0.01285741	0	0.00697658	0	0	0.00825804	0.00278101	0.00666099	0.00853768	0.00553044	0	0.00455911	0.0030836	0	0.02082041	0	0.00262427
13,14-dihydro-15-keto PGD2	0.04834704	0.00998238	0.00162723	0.00546839	0.00189556	0.00537476	0.01599245	0.00789616	0.00666484	0.0107805	0.01515891	0	0.00227298	0	0.00244245	0.01225892	0.00175041	0
PGF2a	0.03029478	0.00848361	0.00318834	0.00894722	0.00526992	0.00342366	0.02811518	0.00521461	0.01039009	0	0.0056297	0.00713767	0.00867168	0.00962842	0	0.01013146	0.00171746	0.00444059
PGE1/D1	0.0047708	0.02794274	0	0.00681215	0	0.00518683	0.01599794	0.00821993	0.02295678	0.00281416	0.02229943	0	0.00658218	0.00961785	0.00618589	0.03967214	0.00548882	0.00763858
8-iso PGF2a	0.0329723	0.00848361	0.00318834	0.00894392	0.00526964	0.00247984	0.02182173	0.00432122	0.00780757	0	0.0056297	0.00601947	0.00746147	0.00769415	0	0.00362795	0.00174637	0.00652314
5-iPF2a-VI	0.01220498	0.01362698	0.00184412	0.00970778	0	0.00353314	0.01108831	0	0.01640537	0	0.01698265	0.00206176	0.00435662	0	0.00444197	0	0.00175036	0
Maresin1	0	0	0	0	0	0	0	0	0	0	0	0	0	0	0	0	0	0
PD1	0	0.00258433	0.00318108	0.00310627	0.0029401	0	0	0.00666235	0	0	0.00562975	0	0.0013633	0.00962882	0.00407104	0.006565	0	0.00241397
TxB2	0.15578249	0.01980041	0.01436194	0.00537447	0.04811491	0.00586518	0.17335966	0.00958853	0.0562911	0	0.01535797	0	0.02116264	0.10979916	0.00296675	0.42155733	0.02836876	0.00853881
6-keto-PGF1a	0	0.00848333	0	0	0.00294026	0	0.00316439	0.01108041	0	0	0	0.00601946	0	0.0032766	0	0.01927389	0.00524866	0.00114938
19/20-OH PGF2a	0	0	0.00162726	0.00402614	0	0.00600204	0.0031643	0	0	0.00281505	0	0.00206177	0	0	0	0	0	0.00340826
RvD1	0	0	0	0	0.00263174	0	0.00311709	0.0020744	0.00286939	0	0	0	0	0.00814485	0	0	0	0
RvD2	0	0	0	0	0	0	0.0069399	0.00207584	0	0.00274752	0.00675513	0	0	0.0032766	0.00144572	0	0	0.00761101
LTE4	0	0	0	0	0	0	0	0	0	0	0	0	0	0	0	0	0	0
LTD4	0.00603215	0	0	0	0.00209026	0	0	0	0	0	0	0	0	0	0	0.00319376	0	0
LTC4	0	0.00374594	0	0.00310614	0	0	0.00251544	0	0	0	0	0	0	0	0.00148337	0	0.00206371	0
PGF1a	0	0.0028265	0.05960986	0.00379564	0	0	0	0	0	0	0.07473816	0.00860168	0.05117547	0	0	0	0	0.06129607
15-keto-PGE2	0.00603215	0	0	0	0	0.00518699	0	0	0	0	0	0	0	0	0	0	0	0
PGD3	0	0.01622295	0.00481326	0.00402611	0.00558118	0	0	0.00562756	0	0	0.00470715	0	0.00240464	0.00327344	0	0.02094648	0	0.00253709
PGA2/PGJ2	0.01048766	0.01085063	0.00318108	0.00703436	0.00153868	0.00336492	0.0054352	0.0081337	0	0.00074161	0.01062494	0.00650242	0.00892767	0.00962882	0	0	0.00116949	0
PGB2	0.00477386	0.00515664	0	0.01023857	0	0	0	0.00262997	0	0.00514772	0	0.00470749	0	0.00327646	0	0.00428663	0.0024919	0
15-deoxy-delta12,14-PGD2	0.00880852	0.00284002	0	0	0.01155394	0.01012046	0.01599827	0.00521788	0	0	0	0.00465665	0.00276347	0.01978713	0.00296673	0.02575126	0.00350073	0.00374253
5,6-DiHETrE	0.0034526	0.00266656	0.01071895	0.01428401	0.06458497	0.00775866	0.04597991	0	0.0105659	0.03623538	0.02660184	0.00935528	0.00465124	0	0.02635985	0.00644169	0	0.00190449
8,9-DiHETrE	0.01894492	0.02246293	0	0.00211861	0.00193267	0	0.00602079	0.01210574	0.01377357	0.02176487	0.02713225	0.02691133	0.0098876	0.03365783	0.01879593	0.00584746	0.02920653	0.00761823
11,12-DiHETrE	0.13832154	0.01530025	0.02961696	0.03621561	0.0679621	0.14266708	0.18449487	0.03568834	0.13386157	0.16961684	0.11246387	0.04509038	0.02393381	0.02095105	0.17118215	0.01979974	0.05983042	0.01741919
14,15-DiHETrE	0.25314244	0.2851802	0.08407026	0.06673701	0.08865614	0.20891383	0.14621531	0.08789911	0.17444377	0.18282615	0.17465069	0.15817538	0.0427578	0.20256671	0.22901717	0.04850597	0.10086025	0.07283636
5-HETrE	0	0.02911327	0.02872587	0.00412028	0	0.02094915	0	0.0354841	0.03483118	0.11552983	0	0.00532609	0	0	0	0	0.04721793	0.01008503
8-HETrE	0.07079045	0.07777401	0.04262773	0.00667031	0	0.05226377	0	0	0.13868969	0.02130126	0.02693501	0	0.03359437	0	0.03115187	0.07847393	0.00846921	0.0417684
15-HETrE	0.12283663	0.1338614	0.03874481	0.0717968	0.07878727	0.14105611	0.04945661	0.41635866	0.32535658	0.32187915	0.91450788	0.05276736	0.33742994	0.04114536	0.0662108	0.36815073	0.26520039	0.02333672
19,20-DiHDPA	0.19657519	0.0148816	0.09533832	0.01938806	0.09466181	0.15260692	0.1294652	0.05666532	0.10466447	0.21054674	0.16100974	0.03036406	0.04923989	0.17368477	0.18713177	0.0622569	0.06385036	0.10421156
2,3-dinor-11beta-PGF2a	0	0	0.00162726	0	0	0	0	0	0	0	0	0	0	0	0	0	0	0
15-deoxy-delta12,14-PGJ2	0	0.03392007	0.01693021	0.00315956	0.01354647	0.03424425	0.02280314	0.00578632	0.01711792	0.01633068	0.04838009	0.01499458	0.00112402	0.02377063	0.01067354	0.00773433	0.00431489	0.00253698
TxB3	0	0	0.00235668	0.00310616	0.00263493	0.00353314	0	0.00655911	0.00801773	0.00654388	0	0.00157938	0	0.00584882	0	0.04531966	0	0
Tetranor-12-HETE	0.01286271	0.02285245	0.00923179	0.03868014	0.02395912	0.07868379	0.06323881	0.02416028	0.02974028	0.09532808	0.05031429	0.02126462	0.09187375	0.02698304	0	0.04328249	0	0.02259983

Precursors	Docosanoids	0.44457102	0.15078243	0.24057397	0.06849294	0.12523814	0.29840486	0.32919493	0.39769005	0.19809762	0.38108731	0.46634915	0.09580794	0.16949095	0.33154691	0.23614217	0.46277348	0.14919596	0.1644754
	Eicosanoids	3.16430801	2.065358	1.35995176	1.21503573	1.24483445	1.68986643	2.3451846	2.42629028	2.37806793	1.94569993	3.00003896	0.95737846	1.52644377	0.91967462	1.04405385	2.54916794	1.32541319	1.11153383
	Octadecanoids	9.30854111	2.84614814	2.19653918	2.17518185	2.91578437	2.21061251	3.52876524	2.51858581	8.65586249	1.81524255	2.23872005	5.16185862	3.24623048	1.15851309	0.92995095	0.62606218	2.91333553	3.76237058
Inflammatory	Anti-inflammatory	7.77025571	3.0421212	2.15121665	2.91924816	3.49962083	2.8753129	4.31060166	3.40145576	8.8932373	3.45884187	3.29394784	4.5228972	3.12171484	1.61600558	1.77581688	1.94358209	2.35996116	6.20284882
	Pro-inflammatory	13.9253286	4.20927298	3.12483579	3.62302841	5.20165711	3.60107252	6.17272985	4.04290409	16.0258439	3.71776977	3.23782076	8.5178867	5.38231456	1.70707805	1.53655225	2.42593049	4.11130551	6.26715966
Enzymatic	COX	0.39802421	0.11483448	0.10184432	0.06980047	0.07050444	0.05878489	0.2740405	0.11924542	0.13405346	0.08429828	0.18105493	0.0779488	0.12147372	0.20968652	0.01914308	0.59547977	0.06969611	0.09098157
	CYP450	14.2303109	4.34536852	3.26474616	3.66621017	5.38027009	3.97172755	6.26394498	4.06039291	16.3664167	4.14311064	3.46957095	8.41098624	5.30341928	2.01566371	2.131215	1.51813757	4.27567713	6.27617438
	LOX	8.2450646	2.92829671	2.30022923	3.25252239	3.81652389	2.91246982	4.69918886	3.41448326	10.2797602	3.3016972	3.06819946	5.27858119	3.55813921	1.36076381	1.37873527	2.82287832	2.59977874	6.80387067

Covariate	p
Age	0.191
FPG	0.507
FPI	0.747
HOMA-IR	0.643
HbA1c	0.48
CrP	0.73
Leptin	0.154
Total.Cholesterol	0.674
HDL.Cholesterol	0.392
LDL.Cholesterol	0.788
Triglycerides	0.0463
ALAT	0.0494
ASAT	0.0274
gGT	0.138

Primer	Sequence	Gene
ARBPfor	TTTGGGCATCACCACGAAAA	ARBP
ARBPrev	GGACACCCTCCAGAAAGCGA	
Ephx1for	GGAGACCTTACCACTTGAAGATG	Ephx1
Ephx1rev	GCCCGGAACCTATCTATCCTCT	
Ephx2for	ACCACTCATGGATGAAAGCTACA	Ephx2
Ephx2rev	TCAGGTAGATTGGCTCCACAG	
Ephx3for	CAGTGGACTCCGATAGCACG	Ephx3
Ephx3rev	TGGGACGACTACAGAGCCG	
Ephx4for	TCCCTGGTGTACGGCTACTG	Ephx4
Ephx4rev	ATCTTAACCCGGAGTCCTTGA	
UCP1for	AGGCTTCCAGTACCATTAGGT	UCP1
UCP1rev	CTGAGTGAGGCAAAGCTGATTT	
LPLfor	GCCCAGCAACATTATCCAGT	LPL
LPLrev	GGTCAGACTTCCTGCTACGC	

Antibody List	Vendor	Catalog #
FATP1(ALSVL5, m-100)	Santa Cruz Biotechnology	sc-25541
Pan-Cadherin(H-300)	Santa Cruz Biotechnology	sc-10733
β-Tubulin	Cell Signaling Technology	2146
HRP conjugated anti Rabbit IgG	Cell Signaling Technology	7074
Anti-CD36	Santa Cruz Biotechnology	sc-9154